NASA
Technical
Paper
2074

October 1982

Flightweight Radiantly and Actively Cooled Panel

Thermal and Structural Performance

Charles P. Shore,
Robert J. Nowak,
and H. Neale Kelly

NASA

NASA
Technical
Paper
2074

1982

Flightweight Radiantly and Actively Cooled Panel

Thermal and Structural Performance

Charles P. Shore,
Robert J. Nowak,
and H. Neale Kelly
Langley Research Center
Hampton, Virginia

National Aeronautics
and Space Administration

**Scientific and Technical
Information Branch**

Certain commercial materials are identified in this paper to specify adequately which materials were investigated in the research effort. Such identification does not imply recommendation or endorsement of the product by NASA, nor does it imply that the materials are necessarily the only ones or the best ones available for the purpose. Equivalent materials are generally available and would probably produce equivalent results.

SUMMARY

A flightweight radiantly and actively cooled panel (RACP) was subjected to thermal/structural tests representing design flight conditions for a Mach 6.7 transport and off-design conditions simulating flight maneuvers and cooling system failures. The 2- by 4-ft RACP was designed to withstand a uniform heat flux of 12 Btu/ft^2-sec to a 300°F surface temperature and utilized René 41 heat shields backed by a thin layer of high-temperature insulation to radiate away most of the incident heating. A 60-percent mass solution of ethylene glycol in water circulating through tubes next to the outer skin of an aluminum-honeycomb-sandwich structural panel absorbed the remainder of the incident heating (0.8 Btu/ft^2-sec). A total of 17 tests exposed the RACP to 53 thermal cycles and multiple cycles of mechanical loading. The RACP successfully withstood 46.7 hr of radiant heating and 5000 cycles of uniaxial inplane limit loading of ±1200 lbf/in. Additionally, the RACP withstood off-design heating conditions for a simulated 2g maneuver from cruise conditions and simulated cooling system failures without excessive temperatures on the structural panel. Previous tests reported in NASA TP-1595 exposed the RACP to 15 aerothermal cycles for a total of 3.5 hr of radiant heating and 137 sec in a Mach 6.6 test stream. The RACP responded as predicted and survived the extensive aerothermal/structural testing imposed by the current tests and those reported in NASA TP-1595 without significant damage to the structural panel, coolant leaks, or hot-gas ingress to the structural panel.

INTRODUCTION

Active cooling of primary structure is one proposed method for coping with the sustained-severe-heating environment which will be encountered by future hydrogen-fueled hypersonic cruise vehicles (refs. 1 to 4). In such systems, a closed-loop secondary cooling circuit with liquid coolant flowing through passages in the surface structure is used to transport the absorbed aerodynamic heating to a heat exchanger where the absorbed heat is transferred to the cryogenic hydrogen fuel flowing to the aircraft engines. By using the heat capacity of the liquid hydrogen fuel, active cooling allows the airframe structure to operate at relatively low temperatures so that conventional materials can be used to obtain long-lived structures. However, it is indicated in reference 5, which summarizes research efforts for actively cooled structures during the 1970's, that the amount of hydrogen heat sink available for airframe cooling depends on engine fuel flow rates and can be insufficient for instantaneous airframe heat loads. Reference 5 also shows that a hot insulation system on the outer surface of a cooled aircraft radiates most of the incident heat back to the atmosphere and reduces the instantaneous heat load to the cooling system to or below the heat-sink capability of the hydrogen flow. Such a system provides the airframe with a thermal response delay that enables deceleration to a less hostile flight velocity if the cooling system fails. Other benefits for the combined radiantly and actively cooled structure include increased safety and reliability, tolerance to off-design conditions, ease of fabrication for the cooled structure, and a small mass reduction compared to a similar structural system with active cooling only.

To assess the thermal and structural performance and the life characteristics of a combined radiantly and actively cooled panel (RACP), a 2- by 4-ft test specimen

with René 41 heat shields backed by a thin layer of insulation and an aluminum-honeycomb structural panel with internal cooling circuits was designed and fabricated under contract for tests in NASA facilities. The RACP (described in ref. 6) incorporates all the essential features of a full-scale 2- by 20-ft RACP designed to withstand a uniform incident heat flux equivalent to 12 Btu/ft^2-sec to a 300°F surface temperature.

As described in reference 7, the RACP was previously subjected to 15 thermal tests, 5 of which combined radiant and aerothermal heating test segments to represent environmental heating conditions at M = 6.6. The RACP withstood 3.5 hr of radiant heating and 137 sec in the test stream and responded to the radiant and aerothermal heating as predicted (i.e., the heat shields reached 1485°F, the cooled panel reached a maximum temperature of 227°F midway between cooling tubes, and the structural panel absorbed heat flux ranged from 0.83 to 1.05 Btu/ft^2-sec). The tests revealed no evidence of coolant leakage or hot-gas ingress which could seriously degrade the RACP performance. In the present investigation, the RACP performance and life characteristics were further evaluated by tests which combined radiant heating with cyclic, uniaxial inplane mechanical loading. The tests also included measurement of the RACP response to a simulated flight maneuver and to simulated cooling system failures.

RADIANTLY AND ACTIVELY COOLED TEST PANEL (RACP)

As shown in figure 1, the RACP features corrugation-stiffened, beaded-skin, René 41 heat shields backed by a thin layer of high-temperature insulation (Min-K[1]) contained within stainless-steel foil packages to seal against water ingress and by an adhesively bonded aluminum-honeycomb-sandwich structural panel with coolant tubes next to the outer skin. The heat shields operate at about 1450°F and reject most of the incident heat by radiation; the remainder (0.8 Btu/ft^2-sec) is absorbed by the structural panel. The structural panel is cooled by a 60-percent mass solution of ethylene glycol in water pumped through the cooling tubes at a flow rate of 3.4 gal/min. Frames representative of typical transport construction support the panel at 2-ft intervals. The test RACP duplicates the essential features of a full-scale 2- by 20-ft RACP, except that the inlet and outlet coolant manifolds located at the ends of the structural panel are only 4 ft apart rather than 20 ft. The heat shield has a longitudinal row of fasteners to simulate a splice between shields and transverse slip joints to allow thermal growth. Figure 2 shows the unit mass for each RACP component. The total unit mass of 4.52 lbm/ft^2 is nearly equally divided between the structural panel (56 percent) and the radiant and active cooling systems (44 percent).

Design Criteria

The test RACP was designed to withstand a uniform incident heat flux equivalent to 12 Btu/ft^2-sec to a 300°F surface temperature. This heating condition corresponds to an aerodynamic heat transfer coefficient of 16 Btu/ft^2-hr-°F and an adiabatic wall temperature of 3000°F, which is representative of the condition at a location 10 ft aft of the nose on the lower fuselage centerline of the Mach 6.7 hydrogen-fueled hypersonic transport shown in figure 3 and described in reference 6.

---

[1]Min-K insulation manufactured by Johns-Manville Corporation.

Additionally, the RACP was also designed to successfully absorb, without coolant flow, the heating from an abort trajectory for the Mach 6.7 hypersonic aircraft described in reference 6. As shown in figure 4, a cooling system failure (no coolant flow) was assumed at the start-of-cruise condition and the aircraft decelerated along a load-factor-limited trajectory subject to the following constraints; a load factor limit of 2.5, an angle-of-attack limit of 20°, a bank angle limit of 40°, and a minimum dynamic pressure of 100 lbf/ft^2.

The RACP was designed to sustain cyclic inplane limit loading of ±1200 lbf/in. on the 2-ft edge and a uniform limit lateral pressure of ±1.0 psi. Cooling tubes in the RACP were designed for a outlet coolant pressure of 50 psi. Design life for the RACP called for 10 000-hr exposure to operational temperatures, 1450°F for the heat shields and 300°F for the aluminum sandwich panel, and 20 000 cycles (5000 cycles with a scatter factor of four) of design limit loads. Stresses in the aluminum sandwich panel were restricted to values below which an initial flaw size of 0.005 in. at the edge of a fastener hole would not grow to a critical length and surface flaws of 0.005 in. would not grow through the thickness of the coolant tubes or manifolds during the 20 000 limit-load cycles. A factor of safety of 1.5 was applied to inplane loads, coolant pressures, and aerodynamic pressure to obtain ultimate loads. The RACP was designed to sustain the design limit loads without yielding and the design ultimate loads without structural failure.

Heat Shields and Insulation Packages

Figure 5 shows some of the design details of the heat shields and insulation packages and also indicates the heat-shield support and attachment scheme. The heat shields consist of a 0.010-in. René 41 beaded outer skin and a 0.010-in. René 41 corrugated inner skin spotwelded together. The insulation packages consist of 16 lb/ft^3 Min-K insulation covered with Astroquartz cloth[2] and packaged in 321 stainless-steel foil. Standoff posts machined from 321 stainless steel are integrated with the insulation packages to support the heat shields. Shoulder bolts machined from alloy A-286 are used to fasten the heat shields and insulation packages to the structural panel. The bolts pass through the heat shields, standoff posts, and structural panel and are retained by plate nuts attached to the inner skin of the cooled panel. (See fig. 1(b).) The shoulders on the bolts provide a controlled gap to prevent clamping of the heat shields and to allow longitudinal thermal expansion of the shields. At the transverse joint, the upstream heat shield overlaps the downstream heat shield. Cutouts in the corrugations and beads allow the upstream heat shield to rest on the downstream shield all along the transverse edge. Slotted holes in the flats between corrugations are sized to accommodate thermal expansion of one-half of each shield. The shields, which are 24.3 in. long, are restrained at midspan and permitted to grow in each direction. Thermal growth in the transverse direction is absorbed by growth of the beads and corrugations.

Structural Panel

As shown in figure 6, the structural panel is an aluminum honeycomb sandwich with D-shaped coolant tubes next to the outer skin. The 6061-T6 aluminum coolant

---

[2]Astroquartz cloth manufactured by J. P. Stevens Company.

manifolds, 6061-T6 aluminum tubes, and 5056-H39 aluminum honeycomb core are adhesively bonded with FM-400[3] adhesive to the 2024-T81 inner and outer skins to form the sandwich (figs. 6(a) and (b)). The manifolds have dual chambers which provide uniform cooling across the panel width (fig. 6(a)). Coolant enters and exits the panel through ports located at opposite ends of the panel at the longitudinal centerline. The coolant flows toward the panel edges in the outer manifold chamber and the manifold ends are cooled as the coolant turns the corners at the panel edges and flows into the inner chamber, where it is distributed into individual coolant tubes. The coolant follows a reversed flow sequence as it exits the panel. To provide close control of the straightness and to obtain bond-line thicknesses of less than 0.010 in., individual tubes were brazed to small tabs which were then bonded to small pockets machined in the manifolds (fig. 6(c)). Close control on the bond-line thickness was required to maintain the high interface conductance between the outer skin and the coolant tubes that is necessary to prevent the structural panel from exceeding the design temperature of 300°F.

Because of cost considerations, the structural-panel manifolds were fabricated as a three-piece weldment rather than an extrusion which would be used in production. To provide proper alignment of the tube/tab assemblies with the manifolds and to minimize adhesive leakage into flow passages during the bonding operation, small neoprene rods were inserted into the coolant passages through holes in the bottom of the manifolds (fig. 6(c)). After the assembly was bonded, the rods were removed and the manifolds sealed with plugs. Proof pressure checks at 190 psi and infrared scans on the completed assembly indicated the coolant flow to be reasonably uniform with no leakage.

Longitudinal and transverse 2024-T81 aluminum splice plates are used to join adjacent panels and to transfer loads from one panel to another in a structural assembly (fig. 6(a)). Both splice plates are mechanically fastened and adhesively bonded to the structural panel. The adhesive provides sufficient conductivity to prevent the splice plates from exceeding the 300°F design temperature and, because the adhesive has a low shear modulus, the fasteners transfer all the loads.

Two methods were used to support the fasteners and to prevent crushing the aluminum honeycomb when installing the fasteners (fig. 6(a), section A-A). In areas under the heat-shield standoff posts where high conductivity is needed to transfer heat away from the bolthead, an aluminum bushing was used. Away from the standoff posts, the honeycomb core was filled locally with a potting compound that cured solid when the skins were bonded to the core. Additional details of the RACP design and fabrication are given in reference 6. Pertinent thermal and mechanical properties (from ref. 6) for the various RACP materials and the coolant are shown in figures 7 and 8 for the metals and the coolant, respectively. Properties for the Min-K insulation and FM-400 adhesive are given in tables I and II, respectively.

INSTRUMENTATION

The RACP was instrumented with thermocouples, strain gages, and thin-foil heat-flux gages. A total of 183 thermocouples of 30-gage chromel-alumel were used to monitor temperatures on the RACP components: 50 on the heat shields, 10 on the insulation packages, and 123 over the surface of the cooled panel (as shown in fig. 9).

---

[3]FM-400 manufactured by American Cyanamid Company.

The thermocouples used on the heat shields were made from stainless-steel-sheathed wire, and junctions on the heat-shield surface were formed by spotwelding the leads to the surface approximately 0.03 in. apart. An expansion loop was formed in the thermocouple wire at each junction to accommodate differential expansion between the sheathed thermocouple wire and the heat-shield surfaces. On the insulation package surfaces, the thermocouple leads were spotwelded to small metal tabs which were then spotwelded to the foil insulation cover. Thermocouples on the heat-shield side of the insulation packages were formed from stainless-steel-sheathed wire and those on the structural-panel side from fiberglass-insulated wire. To avoid possible crack starters from welding or peening, thermocouple junctions for the structural panel were formed by welding the leads together to form a small bead and then bonding the thermocouple to the aluminum skins with a small patch of aluminum adhesive tape covered by a small amount of room-temperature-curing epoxy adhesive with a 400°F temperature limit. Special grade wire with an accuracy of ±2.0°F, exclusive of recording errors, was used for all thermocouples.

Thin-foil heat-flux gages (Micro-Foil[4] Heat Flow Sensor Model 8602) were bonded to the heated surface of the structural panel at locations corresponding to thermocouple locations on the insulation packages. Output from these gages was corrected for temperature effects and was used to monitor the heat-flux distribution over the structural-panel surface. As indicated in figure 9(c), 44 single-arm uniaxial strain gages (Micro-Measurements[5] CEA-13-125 UW-350) were attached to the surfaces of the structural panel to monitor changes in panel skin strains as a function of temperature and applied inplane loading. Pairs of gages were bonded to both surfaces of the cooled panel at the 11 locations shown. A 400°F temperature-limited adhesive was used to bond the strain gages to the panel, then a waterproof epoxy covering was applied to prevent moisture ingress to the gages. At each location, one gage was oriented parallel to the long edge of the panel (inplane loading direction) and one gage perpendicular to the long edge. A single thermocouple was located near each pair of gages and the strain-gage reading was corrected for temperature-induced apparent strain. A three-wire circuit was used to minimize wire-conduction errors, and a four-arm bridge completion circuit was located nearby to minimize lead length errors. The 350-ohm gages were powered by a 5-volt power supply, and each gage circuit was calibrated electrically to obtain the strain sensitivity.

Inlet and outlet coolant temperatures were monitored by chromel-alumel immersion thermocouples with a calibrated accuracy of +0.00°F/-0.31°F. The inlet coolant pressure and the pressure drop through the structural panel were measured by strain-gage-type pressure transducers. The coolant flow rate was monitored by two, calibrated turbine flow meters (for redundancy) located in the flow circuit. For the range of coolant temperatures considered in these tests, viscosity effects on flow-meter readings were insignificant.

---

[4]Micro-Foil is a registered trademark of RdF Corporation.
[5]Division of Measurements Group, Inc.

APPARATUS

Active-Cooling Test Stand (ACTS)

The active-cooling test stand shown in figure 10 consists of three main parts: a bank of air-cooled radiant heaters, a uniaxial fatigue testing machine, and a closed-loop cooling system (not shown). The bank of radiant heaters is mounted vertically on a set of articulated pivots to permit easy access to test panels. A total of 45 quartz tubes, containing 1 to 3 quartz lamps each, are used to provide long-term heating up to 25 Btu/ft^2-sec. Coolant air for the lamps enters from both sides of the lamp bank, exits from a T-junction at the middle of each tube into a manifold at the back of the heater, and is exhausted from the top of the heater. Airflow cools the lamps and electrical connections and is confined to the tube interior only. The number of lamps inside each tube is varied to achieve the desired heating distribution. Since the actual area covered by the quartz lamps is slightly larger than the 2- by 4-ft RACP, water-cooled gold-plated reflectors are used to mask portions of the lamps and provide the desired exposed heated area. A three-phase ignitron-tube power supply is used to power the lamps which were controlled by a closed-loop servo system driven by a water-cooled calorimeter mounted near the bottom of the exposed heater area. The lamp bank was surveyed with a water-cooled calorimeter to determine the lamp distribution and relative power settings of the three phases for the desired heating conditions. The power settings were then adjusted to give nearly uniform temperatures over the RACP heat shields.

The uniaxial fatigue testing machine is hydraulically operated and can impose cyclic loads of ±110 000 lb. Feedback control signals from the load cell are used to achieve cyclic load rates up to 1/2 Hz in the form of a sine-wave load function. Massive grips support the ends of test articles to assure uniform load distribution into the panel ends. Additionally, test panels are supported laterally by three sets of commercially available linear bearings attached to the panel transverse frames. Since the linear bearings are free to move vertically along support rods on either side of the testing machine, the bearings prevent out-of-plane motion of the panel frames but allow unrestrained longitudinal thermal expansion of the panel. Transverse thermal growth is accommodated by slots in the vertical rod supports.

The system shown in figure 11 was used to cool the RACP. The system consists of a 5000-gal storage tank filled with a 60-percent mass solution of ethylene glycol in water, circulation pumps, flow control valves, and a 13.5-ton refrigeration unit (not shown) which chills the coolant solution to 20°F. As shown in the figure inset, independent pumping systems circulate the coolant from the storage tank through the RACP and the refrigeration unit. The flow rate, inlet coolant temperature, and inlet coolant pressure can be independently set by the flow control system.

RACP Installation

Details of the RACP mounting arrangement for ACTS are shown in figure 12. To introduce inplane loads into the RACP, two 1.25-in.-thick aluminum load adapters are attached to the RACP transverse splice plate and the support frame flange by a row of fasteners installed in close-tolerance holes. The load adapters mesh with the massive load grips of the fatigue testing machine shown in figure 10. The load adapters were sized so that the neutral axis of the load adapters and the RACP matched to reduce eccentric loading effects. A strip of asbestos phenolic insulation was placed between the RACP splice plate and support frame and the load adapters to reduce heat loss from the RACP to the load adapters. Section B-B (fig. 12) shows the method of

attachment of the RACP support frames to the fatigue machine lateral support system. To reduce air circulation in the cavity between the heaters and the RACP, flexible high-temperature insulation was packed between the edges of the heater reflector and the edges of the RACP.

TEST PROCEDURES

Thermal and Cyclic Loading

During installation of the RACP in ACTS, the panel was initially hung from the top load grip and not connected to either the lateral supports or the bottom load grip. The strain gages were zeroed, then the RACP was connected to the top and bottom grips and the lateral supports. Strain data were recorded (for no coolant flow or pressure and no inplane load) to obtain the strain distribution due to panel installation. These initial strains represent "clamp-up" strains which were subtracted from all subsequent load-tests strain data. For all thermal tests, the following sequence was used: the fatigue testing machine was turned on and adjusted to take out load due to the support grips; data zeroes were taken; the required coolant flow conditions in the panel were established; and finally, the heaters were brought to operating conditions and allowed to run for approximately 20 min to bring the heater mass to steady-state temperatures. For tests involving inplane loading, the load was cycled at 1/2 Hz. The cyclic loading was interrupted momentarily whenever strain data were recorded. Figure 13 shows a typical temperature history imposed on the RACP heat shields and indicates that the cyclic inplane loading was applied after the panel reached steady-state temperatures. Thermal stress considerations for the heat shields limited temperature rise rates to about 5°F per sec from room temperature. To terminate a test, power to the heaters was reduced so that the heat shields cooled no faster than 5°F per sec until natural cooling occurred at a slower rate, then the heaters were turned off.

Maneuver Heating

To simulate heating conditions during a 2g flight maneuver, temperatures on the heat shield were rapidly increased (in about 8 sec) from 1450°F (design value) to 1740°F (value corresponding to double the design aerodynamic heat-transfer coefficient), maintained for 240 sec, then returned to design values. To determine maximum cooled-panel temperatures for such a maneuver, the simulation was conducted with the coolant temperature corresponding to simulation of the coolant-exit end of a full-scale 2- by 20-ft RACP.

Cooling System Failure Simulation

Since the coolant supply system postulated for the RACP in reference 6 consists of two separate systems, each supplying 50 percent of the required coolant flow to the panel, a possible failure mode is loss of flow in one of the systems. To investigate the RACP response to such a failure, coolant flow through the structural panel was reduced 50 percent for various inlet coolant temperatures. Another failure mode for the RACP is total loss of coolant flow. One method to cope with this problem, predicated on early detection of loss of coolant flow, is to follow a load-factor limited trajectory which minimizes the heat load until flight speeds are decreased to values where aerodynamic heating is negligible (ref. 6). To determine the RACP response to such a procedure, the RACP was subjected to a heating cycle corresponding

to the minimum-heat-load abort trajectory shown in figure 4. The trajectory results in profiles of the aerodynamic heat-transfer coefficient and the adiabatic wall temperature as shown in figure 14. A one-dimensional analysis of transient heat transfer was used to obtain an approximate heat-shield temperature profile also shown in figure 14. In the abort simulation, the RACP was brought to steady-state temperatures corresponding to simulation of the coolant-exit end of a full-scale RACP. At time zero in the abort heating profile, flow through the cooled panel was shut off and the abort heating profile was simulated by adjusting the power to the radiant heaters to obtain the heat-shield temperature profile in figure 14. To minimize heat losses by free convection during the abort simulation, the inner skin of the RACP was covered by insulation, isolated from the massive load grips on the fatigue testing machine, and supported only by the linear bearings attached to the RACP frames.

RESULTS AND DISCUSSION

Summary of Panel Tests

In the present investigation, the RACP was exposed to representative operating conditions in 17 tests. All tests included at least one thermal cycle, and 8 tests combined cyclic inplane loading with the thermal load to investigate the combined thermal/structural performance and life characteristics of the panel. Two tests exposed the RACP to heating representative of a 2g maneuver from design flight conditions. Three tests dealt with the panel's response to cooling system failures; one involved a 50-percent reduction in coolant flow rate at design flight conditions and two involved total loss of coolant flow to the panel under minimum heat input conditions for an abort from design flight conditions shown in figures 4 and 14. A test summary is given in table III. The order of testing, number of thermal cycles, type of test, average heat-shield surface temperature, time at operational temperatures, inlet and outlet coolant temperatures, average coolant flow rate, and absorbed heat flux are included in the table. In the tests, the heat-shield surface temperature ranged from 1430°F to 1740°F, the inlet coolant temperature was varied from 47°F to 130°F and the absorbed heat flux ranged from 0.65 Btu/ft^2-sec to 0.84 Btu/ft^2-sec. During the test program, the RACP was exposed to operational temperatures for 46.7 hr, to 53 thermal cycles, and to 5000 inplane limit-load cycles of ±1200 lbf/in.

RACP Thermal/Structural Performance

Thermal loading.- Basic questions regarding the thermal performance of the RACP and its use to represent the thermal performance of a full-scale 2- by 20-ft RACP were answered in the investigation described in reference 7. Results presented in reference 7 indicate that the RACP responded to radiant and aerothermal heating as predicted in reference 6. The current investigation was directed toward questions about the combined thermal/structural performance of the RACP and its response to off-design thermal conditions and to simulated cooling system failures. Hence, only limited results regarding RACP thermal performance at design heating conditions are presented to show that the structural panel was operating at the required thermal conditions during the combined thermal/structural tests. Figure 15 shows a comparison of typical longitudinal temperature distributions from the current tests (test 8) and from reference 7 for similar test conditions. The current experimental results agree well with those from reference 7 although temperatures on the structural panel from the current tests were about 10°F to 15°F cooler than those from the tests of reference 7. This difference can be attributed to differences in the exper-

imental setup between the two series of tests. In the tests of reference 7, the RACP was mounted horizontally in a well-sealed, fully enclosed cavity with higher ambient temperatures than in the current tests where the RACP was mounted vertically with the inner skin of the structural panel exposed to cooler ambient air. Additionally, heat losses from free convection over the RACP surfaces can be expected to be greater in the current tests because such losses are larger for vertically mounted plates. A calculated estimate indicated the convective heat loss from the inner skin to be 0.042 Btu/ft^2-sec, or 5 percent of the absorbed heat flux. Results from tests 16 and 17 revealed that insulating the inner skin of the structural panel raised inner skin temperatures about 15°F and outer skin temperatures about 5°F.

Predicted temperatures from reference 6 are shown in figure 15 by the shaded bands for the heat shields and the structural panel. The temperatures were obtained from a three-dimensional, finite-difference thermal analysis of the RACP. The upper bound for the heat shield represents temperatures between the beads, and the lower bound represents temperatures on the bottom of the corrugations. The upper bound for the structural panel represents temperatures for regions near fasteners which penetrated the panel, and the lower bound represents temperatures on the outer skin midway between coolant tubes. Both sets of measured temperatures for the structural panel are slightly less than the predicted temperatures from reference 6; however, the predicted temperatures are expected to be higher than measured values since the predicted temperatures are based on no heat loss from the RACP inner skin.

Cyclic loading.- As indicated in table III, the RACP was subjected to 5000, uniaxial, inplane load cycles of ±28 800 lbf (design limit load). The load cycles were applied under thermal conditions which produce temperatures corresponding to those expected near the coolant-exit (region of highest temperature) end of a full-scale RACP. Table IV contains measured structural panel strains at design limit loads for room and operational temperatures before and after the 5000 load cycles were applied. Although there is considerably more scatter in the transverse strains, they fall within values expected from Poisson's effect for uniaxial loading. Comparison of the longitudinal strains indicates that the change in measured strains for room and operational temperatures is generally less than 10 percent, with 90 percent of the data within 3.5 percent. The good agreement of the strains measured before the 5000 load cycles with those measured afterward indicates that, although a 0.9-in. crack was induced at a corner fastener hole in a longitudinal splice plate, the load carrying ability of the structural panel was not degraded by exposure to the cyclic loading.

The strains measured along the centerline near the coolant inlet and outlet (given in table IV) were converted to stresses which are compared to predicted stresses from a finite-element stress analysis of the RACP (ref. 6) in table V for room and operational temperatures. The measured stresses agree reasonably well (within 17 percent) with the predicted stresses, although it appears that the coolant tubes may be carrying slightly more load than predicted since the stresses in the outer skin are somewhat lower than predicted.

Maneuver heating.- Results from the simulated maneuver-heating tests described in the section entitled Test Procedures are shown in figures 16 and 17. Figure 16 shows the applied heat pulse in terms of the percentage change from design conditions. The history of the heat flux to the structural panel measured by the thin heat-flux gage bonded to the outer skin near the coolant-exit end of the panel and the absorbed-heat-flux history are also shown. The absorbed-heat-flux response is slower than that measured on the structural-panel outer skin because of the thermal

mass of the structural panel and the coolant. The lag due to thermal mass prevented the structural panel and coolant from reaching equilibrium during the 240-sec heat pulse. Figure 17 shows the temperature response at various points through the depth of the RACP. Also shown for comparison is a calculated temperature response from reference 5 for an unshielded, actively cooled panel (ref. 8) designed for the RACP aerodynamic heating conditions. The increase in heating causes the heat-shield temperature to increase to 1740°F, a change of 290°F from normal operation. However, the structural-panel temperature only increases 30°F compared to a 130°F predicted increase for an unshielded actively cooled panel. Thus, the RACP is relatively insensitive to off-design thermal conditions compared to an unshielded actively cooled panel designed for the same aerodynamic heating environment.

Reduced-coolant-flow failure simulation.- Figure 18 shows the structural-panel temperature response to a 50-percent reduction in coolant flow rate as a function of inlet coolant temperature. The outlet coolant temperature and the temperature along the structural-panel centerline midway between cooling tubes at two locations, one 6 in. from the coolant inlet and the other 6 in. from the coolant outlet, are shown for the design flow rate and for 50 percent of the design flow rate. Analytical predictions from a three-dimensional finite-difference thermal analysis described in reference 6 are shown for comparison. The measured temperatures agree reasonably well with the predicted temperatures but are somewhat lower. However, the measured temperatures are expected to be lower than predicted values since the predicted temperatures do not include heat losses due to convection currents around the RACP. The 50-percent reduction in coolant flow rate results in a temperature increase near the coolant outlet of only about 20°F which corresponds to the predicted increase. Again this illustrates the insensitivity of the RACP to off-design operating conditions.

No-coolant-flow failure simulation.- Shown in figure 19 are temperature histories of the RACP response to the abort heating simulation, test 17, for the heat shields and cooled panel. Average measured heat-shield and structural-panel temperatures are shown. Also shown for comparison are heat-shield and structural-panel temperature histories from a one-dimensional transient heat-transfer analysis for the abort heating profile starting at steady-state conditions. A calculated response for an unprotected aluminum panel is also shown. Maximum temperature for the RACP structural panel reached about 325°F, only 25°F above the panel maximum design temperature indicated by the tic mark on the ordinate. Thus, the RACP appears to tolerate the abort heating profile very well. By comparison an unprotected panel would very quickly reach temperatures where aluminum has virtually no strength.

RACP Posttest Condition

Heat shields.- Except for some slight discoloration over the heat-shield surface which was noticed following the aerothermal tests described in reference 7, the outer heat-shield surface was in excellent condition at the conclusion of the current tests. Figure 20(a) shows the posttest appearance of the heat-shield outer surface. The light-shaded rub marks at the center slip joint indicate that the heat shields moved about 0.25 in. when heated to test temperatures. This value is consistent with calculated values for the 1420°F temperature change from ambient conditions. There was no evidence of excessive wear or binding at the slip joint as a result of the 53 thermal cycles and the 5000 inplane load cycles imposed on the RACP. Additionally, there was no evidence of buckling of the heat-shield skins. Figure 20(b) shows the posttest appearance of the inner surface of the heat shields. Except for the two cracks in the elongated fastener holes of the center slip joint at the outer edges of

the panel, there was no evidence of damage to the inner heat-shield surface. The cracks may have resulted from embrittlement of the René 41 material or excessive stresses imposed by interference with the attachment bolts caused by high temperatures during the maneuver heating tests.

Insulation packages.- The posttest condition of the insulation packages is shown in figure 21. As shown in figure 21(a), the foil surface next to the heat shields was severely wrinkled and oxidized as a result of the tests. The wrinkles were sufficient to tear the foil in some areas. As shown in figure 21(b), the foil surface next to the structural panel did not oxidize and was much less wrinkled than the surface next to the heat shields. However, there were patches of discoloration with numerous small holes scattered over the inner foil surface. The holes do not appear to result from rubbing or excessive wear, but rather appear to result from some localized chemical attack. Spectrographic and microscopic examination of the material surrounding the holes indicated that the corrosion occurred from the inside (surface next to the insulation) and apparently resulted from chloride contamination. The appearance of the degraded areas is indicative of local corrosive attack similar to laboratory crevice erosion failures. The source of the contamination was not apparent; the insulation was free of chlorides and there was no evidence of any sodium concentration. It is postulated that the corrosion did not occur on the higher-temperature surface because the higher temperatures drove off any aqueous solution required for the chemical reactions to occur. In any event, damage to the foil insulation packages appears sufficient to destroy their function of preventing water ingress to the layer of high-temperature insulation.

Structural panel.- The posttest appearance of the structural panel is shown in figure 22. Except for some areas of discolorations on the outer surface corresponding to those noted on the insulation packages and the 0.9-in. crack in the longitudinal splice plate at a corner fastener hole, the structural panel sustained no significant damage as a result of the extensive testing imposed by the current thermal/structural tests and the aerothermal tests described in reference 7. It should be noted that, during the RACP installation in ACTS, the structural panel was inadvertently loaded without the heat-shield fasteners in place and the splice-plate adhesive bond at the corner fastener hole was destroyed. Thus, during the subsequent cyclic load tests, the possibility existed for flexing of the splice plate to occur at the fastener hole leading to increased possibilities for crack growth in the splice plate. Extensive X-ray examination of the structural panel before and after the tests indicated that there was no evidence of internal cracks or coolant leakage nor was there any external signs of coolant leakage at any time during the entire sequence of tests.

CONCLUDING REMARKS

A flightweight radiantly and actively cooled panel (RACP) applicable to hydrogen-fueled hypersonic aircraft was subjected to repeated radiant heating tests and to cyclic inplane loading to design limit loads to evaluate the RACP thermal/structural performance and design life characteristics. Additionally, the RACP was subjected to heating conditions associated with a maneuver from design flight conditions and to reduced coolant flow tests to determine the RACP response to off-design conditions. Finally, to determine survivability, the RACP was subjected to a simulated abort maneuver which consisted of stopping coolant flow through the panel and applying a heating profile representative of a minimum-heat-load descent from design flight conditions.

The 2- by 4-ft RACP incorporated all the essential features of a full-scale 2- by 20-ft radiantly and actively cooled panel designed to withstand a uniform incident heat flux equivalent to 12 Btu/ft^2-sec to a 300°F surface temperature. The RACP featured corrugation-stiffened, beaded-skin René 41 heat shields backed by a thin layer of high-temperature insulation contained within a stainless-steel foil package to reject most of the incident heat by radiation. An adhesively bonded structural panel which consists of an aluminum-honeycomb-sandwich structure with half-rounded coolant tubes next to the outer sandwich skin carries the structural load and absorbs the remainder of the incident heat (0.8 Btu/ft^2-sec). A 60-percent mass solution of ethylene glycol in water was used to cool the RACP. Frames representative of typical transport aircraft construction supported the RACP at 2-ft intervals. The RACP was subjected to 17 thermal tests, 8 of which combined cyclic inplane loading to design limit loads. The tests imposed a total of 53 thermal cycles and 5000 inplane load cycles at operating temperatures over a total of 46.7 hr of operation at thermal design conditions.

The current thermal/structural tests combined with the aerothermal tests described in NASA TP-1595 exposed the RACP to 50 hr of design heating conditions, 68 thermal cycles, 137 sec in a Mach 6.6 aerothermal environment, 5000 inplane load cycles of ±1200 lbf/in., a simulated 2g maneuver from flight conditions, reduced coolant flow at design heating conditions, and finally, a simulated abort (no coolant flow) from design flight conditions. The tests revealed that the RACP responded to radiant and aerothermal design heating conditions as predicted: the heat shields reached 1485°F, the cooled panel reached a maximum temperature of 227°F midway between coolant tubes, and the structural-panel absorbed heat flux ranged from 0.65 to 1.05 Btu/ft^2-sec. The measured thermal and structural performance agreed within 17 percent of the predicted performance for design heating and loading conditions. Responses to off-design heating associated with a 2g flight maneuver, to reduced coolant flow at design heating conditions, and to simulated abort heating conditions were within acceptable limits. Except for the foil covering on the insulation which sustained damage sufficient to destroy its ability to prevent water ingress, the RACP survived the extensive thermal/structural testing with no significant structural failures and no evidence of coolant leaks.

Langley Research Center
National Aeronautics and Space Administration
Hampton, VA 23665
August 24, 1982

REFERENCES

1. Becker, John V.: New Approaches to Hypersonic Aircraft. Paper presented at the Seventh Congress of the International Council of the Aeronautical Sciences (Rome, Italy), Sept. 1970.

2. Helenbrook, R. G.; and Anthony, F. M.: Design of a Convective Cooling System for a Mach 6 Hypersonic Transport Airframe. NASA CR-1918, 1971.

3. Anthony, F. M.; Dukes, W. H.; and Helenbrook, R. G.: Internal Convective Cooling Systems for Hypersonic Aircraft. NASA CR-2480, 1975.

4. Pirrello, C. J.; Baker, A. H.; and Stone, J. E.: A Fuselage/Tank Structure Study for Actively Cooled Hypersonic Cruise Vehicles - Summary. NASA CR-2651, 1976.

5. Kelly, H. Neale; Wieting, Allan R.; Shore, Charles P.; and Nowak, Robert J.: Recent Advances in Convectively Cooled Engine and Airframe Structures for Hypersonic Flight. Recent Advances in Structures for Hypersonic Flight, NASA CP-2065, Part I, 1978, pp. 47-61.

6. Ellis, D. A.; Pagel, L. L.; and Schaeffer, D. M.: Design and Fabrication of a Radiative Actively Cooled Honeycomb Sandwich Structural Panel for a Hypersonic Aircraft. NASA CR-2957, 1978.

7. Shore, Charles P.; and Weinstein, Irving: Aerothermal Performance of a Radiatively and Actively Cooled Panel at Mach 6.6. NASA TP-1595, 1979.

8. Koch, L. C.; and Pagel, L. L.: High Heat Flux Actively Cooled Honeycomb Sandwich Structural Panel for a Hypersonic Aircraft. NASA CR-2959, 1978.

TABLE I.- INSULATION PROPERTY DATA

Material	High-temp. flexible Min-K
Description	Proprietary silica-based material
Density, lbm/ft^3	16
Thermal conductivity, $Btu\text{-}in/hr\text{-}ft^2\text{-}°F$ at 1000°F	0.36
Minimum available thickness, in.	0.125
Maximum continuous use, °F	1800
Vendor	Johns-Manville
Characteristics	Flexible with moderate load bearing capability

TABLE II.- ADHESIVE PROPERTY DATA

Bonding material	Exposure		Test temp., °F	Peel strength, lbf/in.	Shear strength, ksi	Thermal conductivity, $Btu\text{-}in/hr\text{-}ft^2\text{-}°F$
	Time	Temp., °F				
FM-400	None	None	75	19.0	3.44	2.6
	10 min	-67	-67		3.56	2.6
	18 hr	365	75		4.03	2.6
	18 hr	365	365	7.2	3.08	2.6
	3 hr	420	420		1.82	2.6

TABLE III.- TEST SUMMARY

Test	Number of thermal cycles	Type of test	Average heat shield temperature, °F	Time at operational temperatures, hr	Coolant temperature		Average flow rate, gal/min	Absorbed heat flux, Btu/ft^2-sec	Comments
					Inlet, °F	Outlet, °F			
1	2	Check out	1500	4.80					Heater and instrumentation check outs
2	2	Cyclic load*	1500	1.80	130	144	3.46	0.72	Load cycles 1 to 8
3	1	↓	1500	.72	50	67	3.39	.81	Load cycles 9 to 10
4	1	↓	1475	3.33	128	142	3.50	.72	Load cycles 11 to 13
5	1	↓	1495	2.21	94	110	3.40	.79	Load cycles 14 to 17
6	6	↓	1480	2.14	126	140	3.43	.71	Load cycles 18 to 490
7	1	↓	1480	1.27	128	143	3.47	.77	Load cycles 491 to 1000
8	10	↓	1465	5.23	128	143	3.47	.77	Load cycles 1001 to 3500
9	3	↓	1490	2.32	128	143	3.47	.77	Load cycles 3501 to 5000
10	10	Thermal	1430	1.88	47 to 130	62 to 143	3.39	0.72 to 0.65	Inlet temperature variation
11	1	↓	1515	1.90	50 to 125	67 to 140	3.36	.80 to .69	↓
12	6	↓	1550	6.61	52 to 125	70 to 139	3.36	.84 to .69	↓
13	1	Maneuver heating	1740 (peak)	1.47	51 to 127	68 to 144	3.40	.85 to .75	2g maneuver heating for 4 min
14	3	Maneuver heating	1740 (peak)	2.95	51 to 125	67 to 139	3.33	.78 to .69	2g maneuver heating for 4 min
15	1	Coolant failure	1550	2.60	50 to 114	84 to 144	1.67	.79 to .69	50% design flow rate
16	3	Abort	1650 (peak)	2.45					Abort heating profile
17	1	Abort	1650 (peak)	2.97					Abort heating profile
Total	53		Total time	46.65					

*Cyclic load = ±28 800 lb.

TABLE IV.- COOLED-PANEL STRAINS FOR ±28 800 lbf

(a) Room temperature

Gage	Microstrain at 28 800 lbf				Microstrain at -28 800 lbf			
	Temp., °F	No cycles	5000 cycles	Change, percent	Temp., °F	No cycles	5000 cycles	Change, percent
1	74	-253	-258	2.0	62	275	283	2.9
2	↓	939	948	1.0	↓	-999	-1013	1.4
3		-291	-290	-.3		304	298	-2.0
4		1206	1208	.2		-1264	-1221	-3.4
5		-211	-214	1.4		187	210	12.3
6		951	983	3.4		-977	-1046	7.1
7		-212	-213	.5		189	214	13.2
8		1183	1197	1.2		-1129	-1118	-1.0
9		-258	-252	-2.3		263	265	.8
10								
11		-281	-279	-.7		286	283	-1.0
12		1212	1218	.5		-1199	-1166	-2.8
13		-356	-355	.3		363	366	.8
14		1063	1065	.2		-1070	-1068	-.2
15		-343	-349	1.7		340	353	3.8
16		1190	1209	1.6		-1205	-1205	0
17		-381	-370	-2.9		363	363	0
18		1147	1131	-1.4		-1155	-1146	-.8
19		-295	-287	-2.7		265	264	-.4
20		1070	1073	.3		-1075	-1094	1.8
21		-416	-403	-3.1		401	403	.5
22		1121	1121	0		-1125	-1128	.3
23		-325	-312	-4.0		297	322	8.4
24		1127	1138	1.0		-1138	-1152	1.2
25		-374	-372	-.5		356	357	.3
26		1119	1142	2.1		-1139	-1116	-2.0
27		-314	-294	-6.4		286	275	-3.8
28		1045	1071	2.5		-1047	-1067	1.9
29		-366	-361	-1.4		367	365	-.5
30		1110	1131	1.9		-1107	-1114	.6
31		-340	-337	-.9		342	352	-2.8
32		1207	1207	0		-1220	-1227	.6
33		-293	-287	-2.0		296	292	-1.4
34		1061	1078	1.6		-1084	-1079	-.5
35		-326	-312	-4.3		334	336	.6
36		1264	1224	-3.2		-1279	-1272	-.5
37		-213	-223	4.7		201	216	7.5
38		989	1018	2.9		-992	-1011	1.9
39		-179	-123	-31.3		189	191	1.1
40		1159	1043	-10.0		-1156	-1125	-2.7
41		-265	-267	.8		260	256	-1.5
42		1000	1013	1.3		-998	-1002	.4
43		-293	-300	2.4		277	279	.7
44	↓	1244	1276	2.6	↓	-1219	-1201	-1.5

TABLE IV.- Concluded

(b) Heated

Gage	Microstrain at 28 800 lbf				Microstrain at -28 800 lbf			
	Temp., °F	No cycles	5000 cycles	Change, percent	Temp., °F	No cycles	5000 cycles	Change, percent
1	190	-303	-316	4.2	186	273	271	-0.6
2	190	913	922	1.0	186	-1188	-1211	1.9
3	146	-319	-320	.1	143	311	303	-2.7
4	146	1313	1335	1.6	143	-1285	-1233	-4.1
5	184	-282	-314	11.5	181	152	133	-12.1
6	184	989	1012	2.4	181	-1088	-1154	6.1
7	143	-219	-254	16.0	141	212	193	-8.8
8	143	1334	1356	1.7	141	-1092	-1065	-2.5
9	180	-328	-319	-2.7	179	239	247	3.5
10	180				179			
11	144	-317	-330	4.1	141	282	277	-1.8
12	144	1423	1421	-.2	141	-1097	-1093	-.4
13	204	-535	-507	-5.2	198	237	279	17.9
14	204	1255	1237	-1.4	198	-1054	-1113	5.5
15	167	-490	-483	-1.5	164	236	260	10.1
16	167	1377	1371	-.5	164	-1191	-1197	.5
17	216	-330	-334	1.4	207	476	465	-2.2
18	216	1038	1056	1.7	207	-1375	-1354	-1.5
19	182	-284	-291	2.3	170	255	247	-3.2
20	182	1175	1208	2.9	170	-1112	-1087	-2.3
21	216	-405	-404	-.3	208	451	454	.8
22	216	1129	1141	1.1	208	-1265	-1260	-.4
23	175	-356	-346	-2.7	168	299	321	7.4
24	175	1322	1311	-.8	168	-1101	-1129	2.5
25	216	-410	-411	.3	207	390	385	-1.2
26	216	1163	1151	-1.0	207	-1217	-1227	.8
27	185	-339	-331	-2.5	170	260	253	-2.7
28	185	1266	1270	.3	170	-1017	-1028	1.0
29	214	-470	-417	-11.3	207	309	361	16.9
30	214	1234	1203	-2.5	207	-1143	-1186	3.8
31	183	-500	-479	-4.3	177	231	259	11.9
32	183	1370	1355	-1.1	177	-1254	-1254	0
33	209	-445	-423	-5.0	204	178	191	6.9
34	209	1060	1078	1.7	204	-1200	-1197	-.3
35	166	-379	-371	-2.1	163	312	307	-1.4
36	166	1395	1391	-.3	163	-1263	-1226	-2.9
37	212	-475	-470	-1.2	205	-38	-15	-60.4
38	212	1038	1040	.2	205	-1050	-1092	4.0
39	163	-236	-199	-15.7	159	122	108	-11.7
40	163	1261	1165	-7.6	159	-1088	-1067	-1.9
41	212	-502	-485	-3.3	206	65	95	46.2
42	212	1078	1065	-1.2	206	-1066	-1126	5.6
43	165	-375	-376	.4	160	220	239	8.6
44	165	1437	1459	1.5	160	-1128	-1139	.9

TABLE V.- COMPARISON OF MEASURED AND PREDICTED LIMIT-LOAD STRESSES FOR COOLED PANEL

Strain gage	Measured		Predicted	
	Room-temperature stress, ksi	Operational-temperature stress, ksi	Room-temperature stress, ksi	Operational-temperature stress, ksi
Tension load - 28 800 lbf				
6	10.4	10.5	12.5	11.2
8	13.1	14.7	12.7	13.3
38	10.8	10.3	12.5	11.4
40	12.9	13.9	12.7	13.3
Compression load - 28 800 lbf				
6	10.8	12.1	12.5	13.8
8	12.5	11.9	12.7	13.3
38	10.9	12.2	12.5	13.6
40	12.9	12.2	12.7	13.3

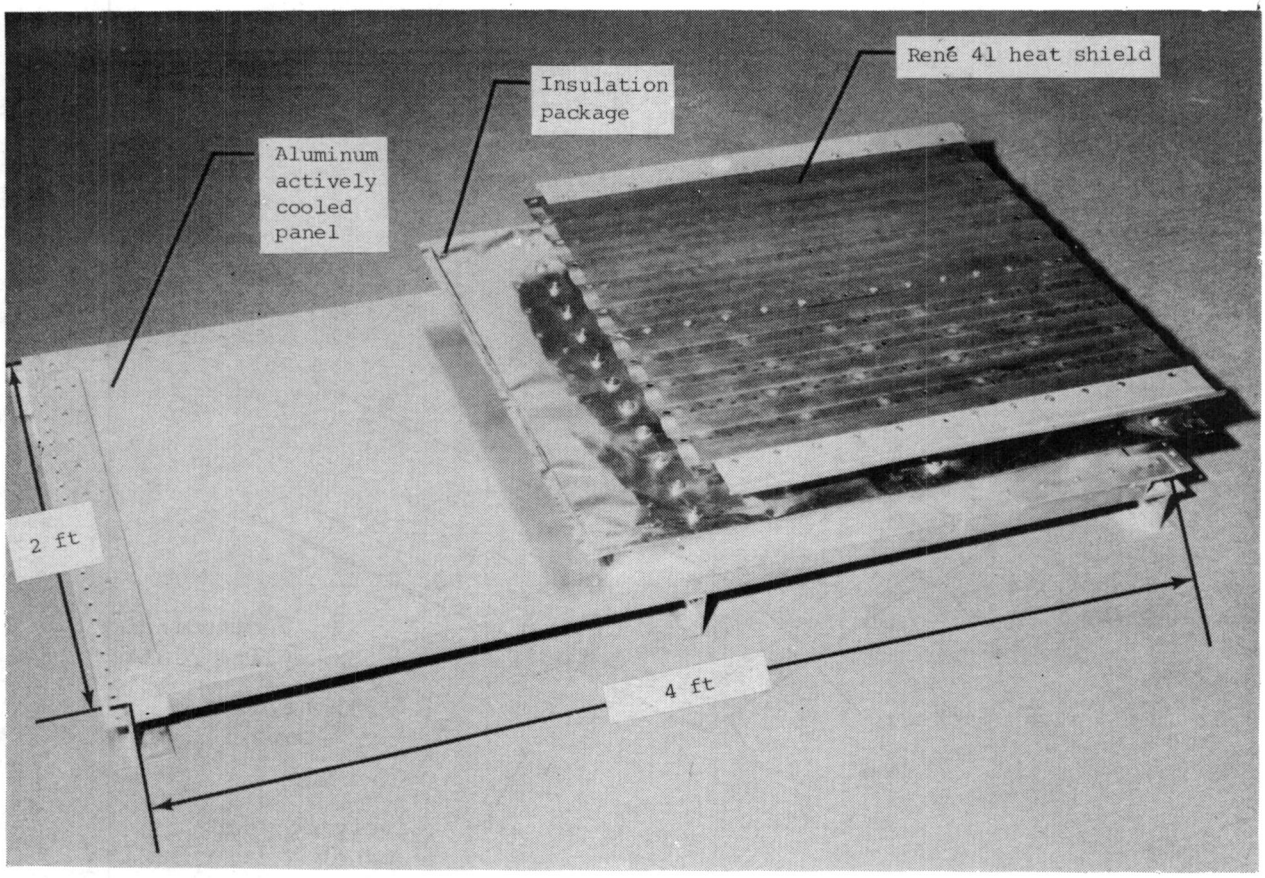

L-79-352.2

(a) Components of RACP test panel.

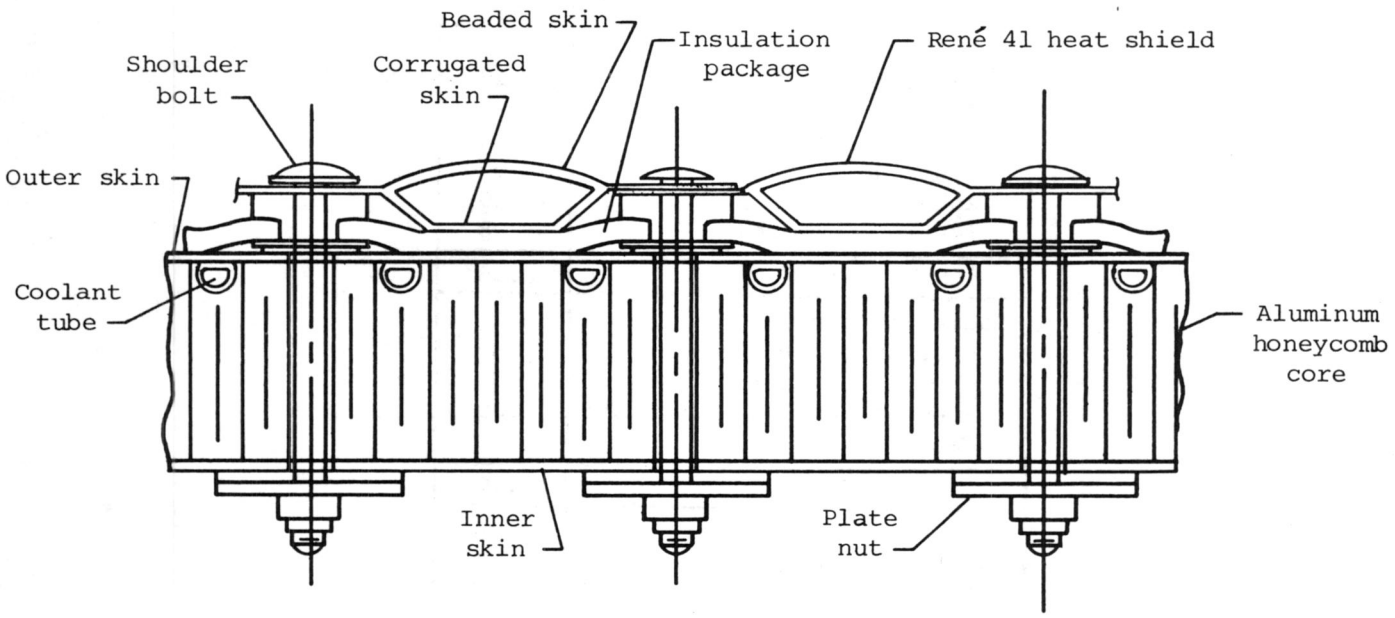

(b) Cross section of RACP.

Figure 1.- Radiantly and actively cooled panel (RACP).

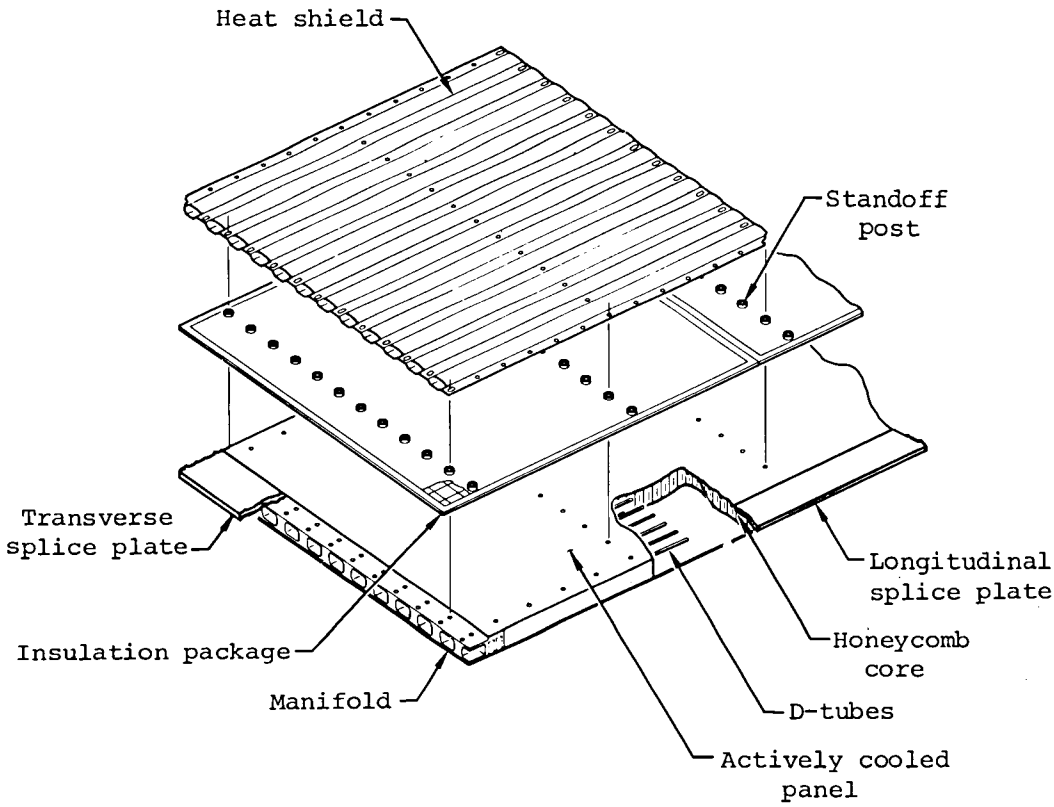

Component	Unit mass, lbm/ft^2
Structural panel	
Skins (2024-T81)	1.20
D-tubes (6061-T6)	.16
Honeycomb (5056-H39)	.29
Manifolds (6061-T6)	.13
Splice plates (2024-T81)	.13
Bushings/Fasteners	.13
Plumbing	.03
Adhesives	.40
Potting compound	.08
Subtotal	2.55
Radiation system	
Heat shield (René 41)	.89
Insulation package	.38
Support posts (321 Stn Stl)	.09
Fasteners (A-286)	.13
Subtotal	1.49
Active cooling system	.28
Panel fluid penalties	.20
Total	4.52

Figure 2.- Masses of radiantly and actively cooled panel components.

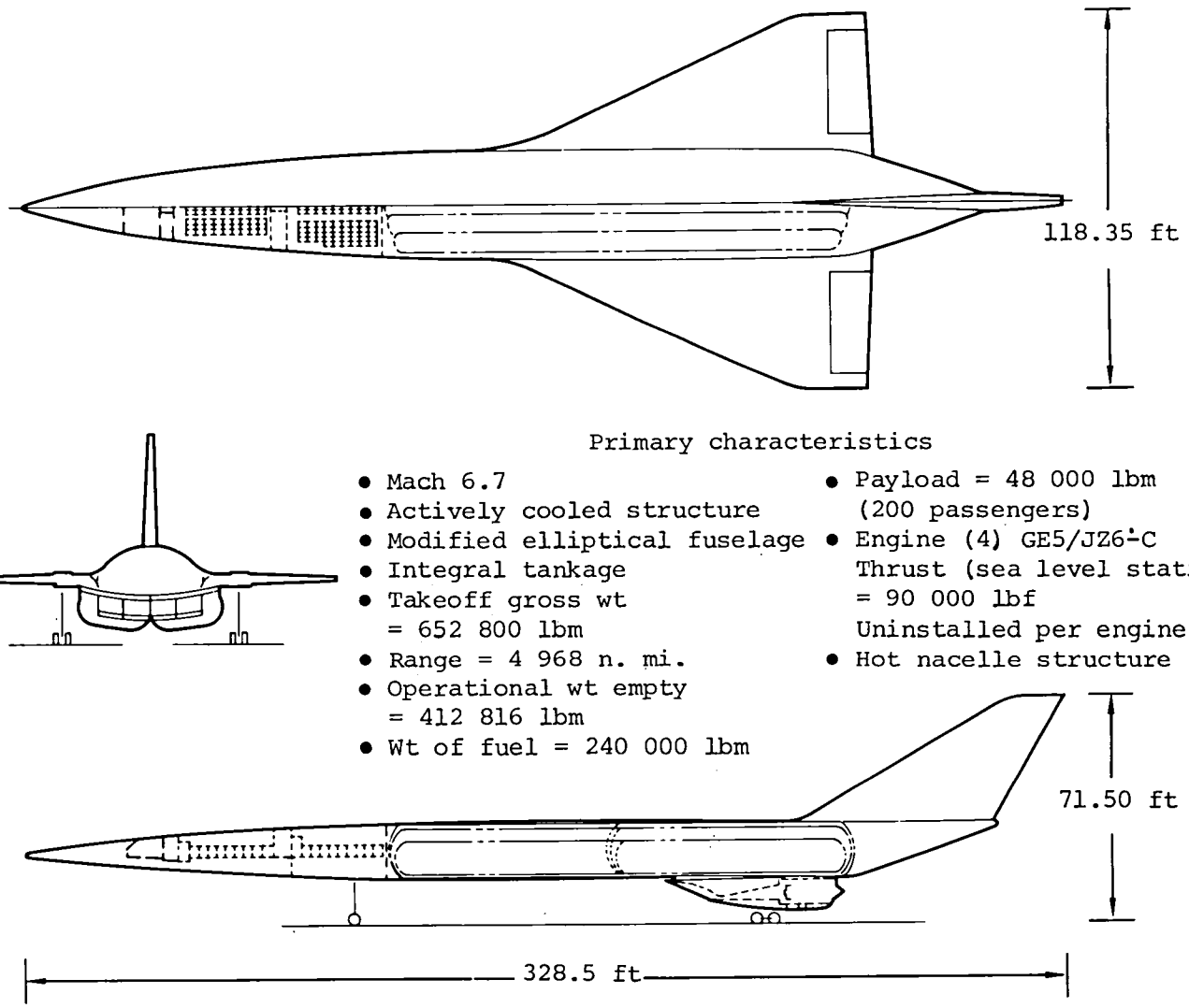

Figure 3.- Baseline aircraft.

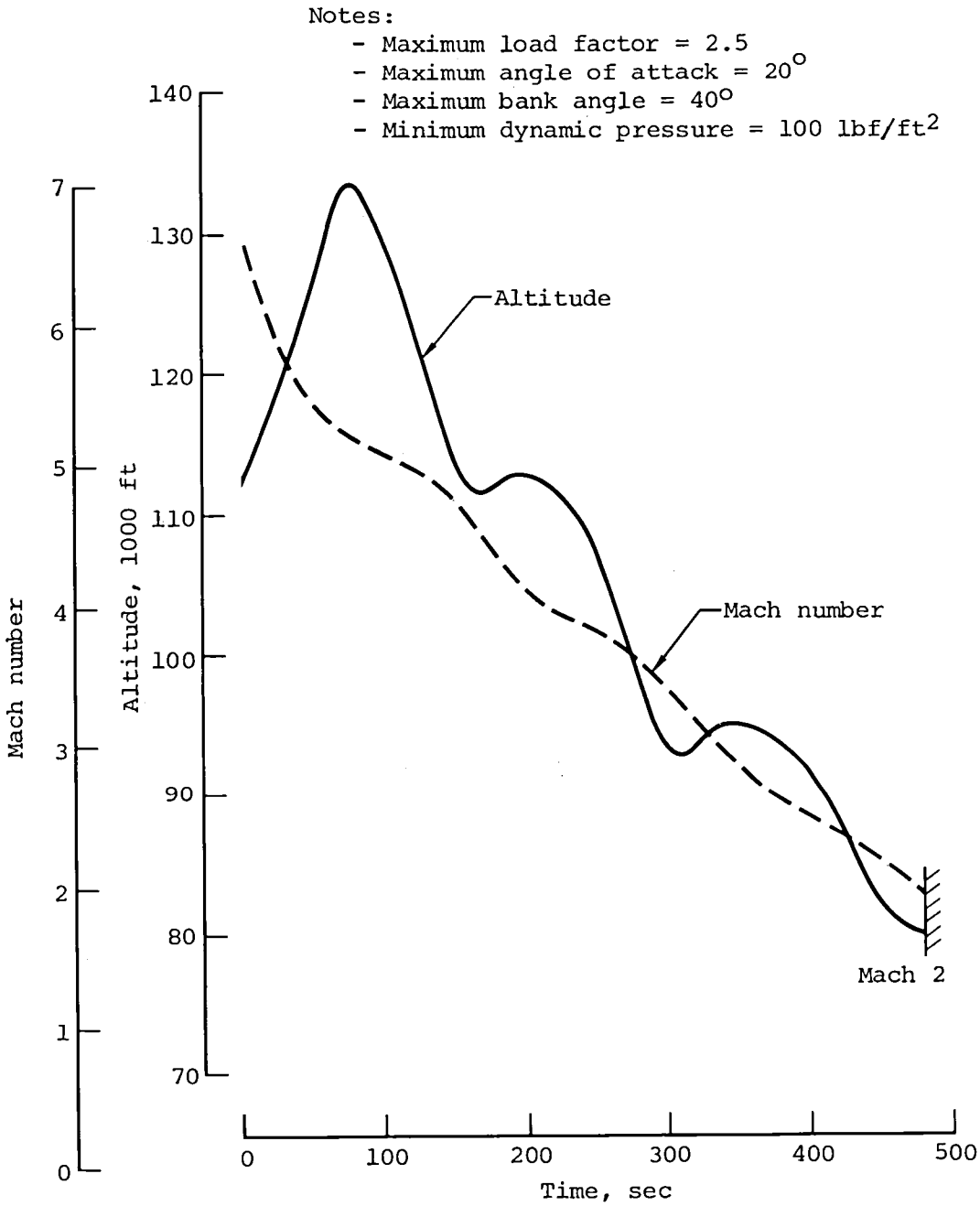

Figure 4.- Abort trajectory.

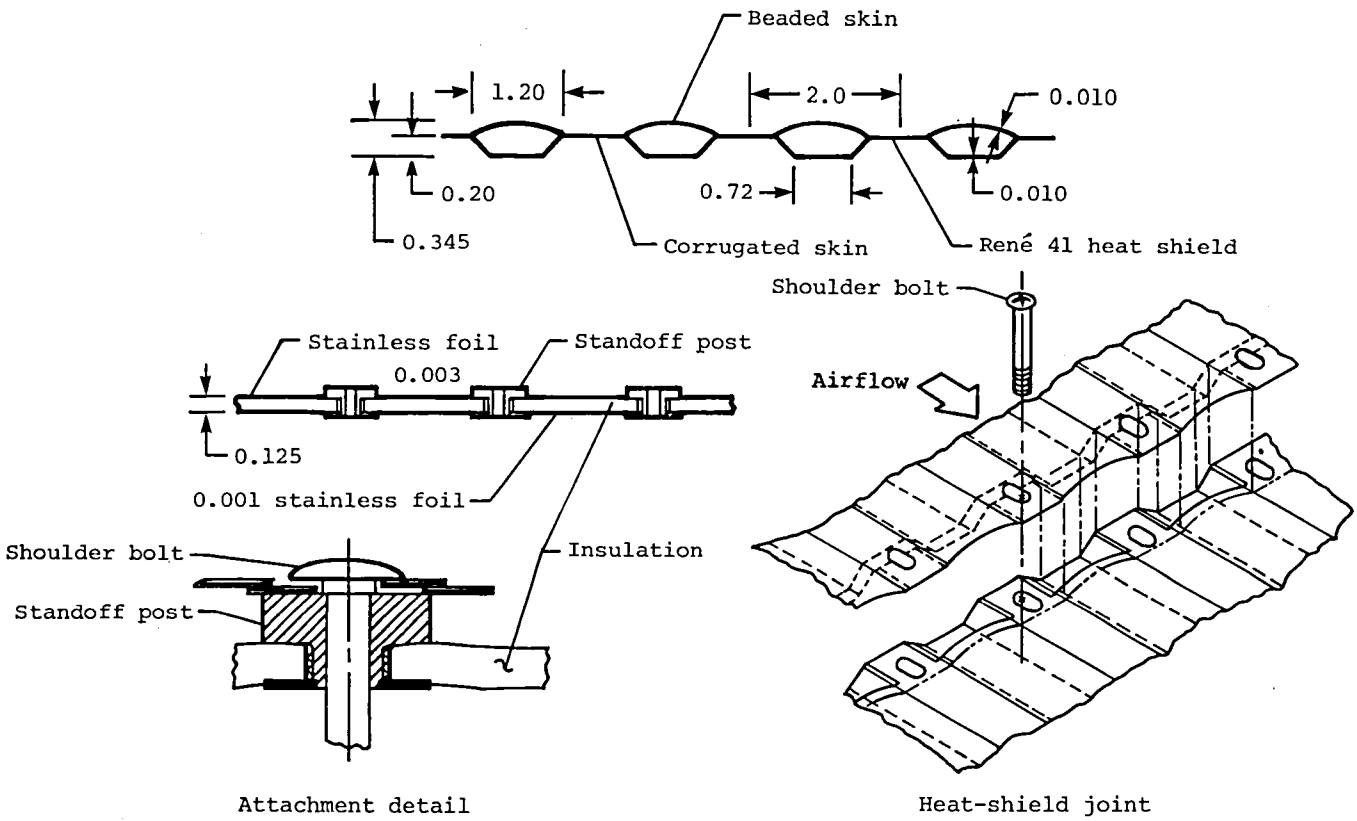

Figure 5.- Details of heat shield and insulation. Dimensions are in inches.

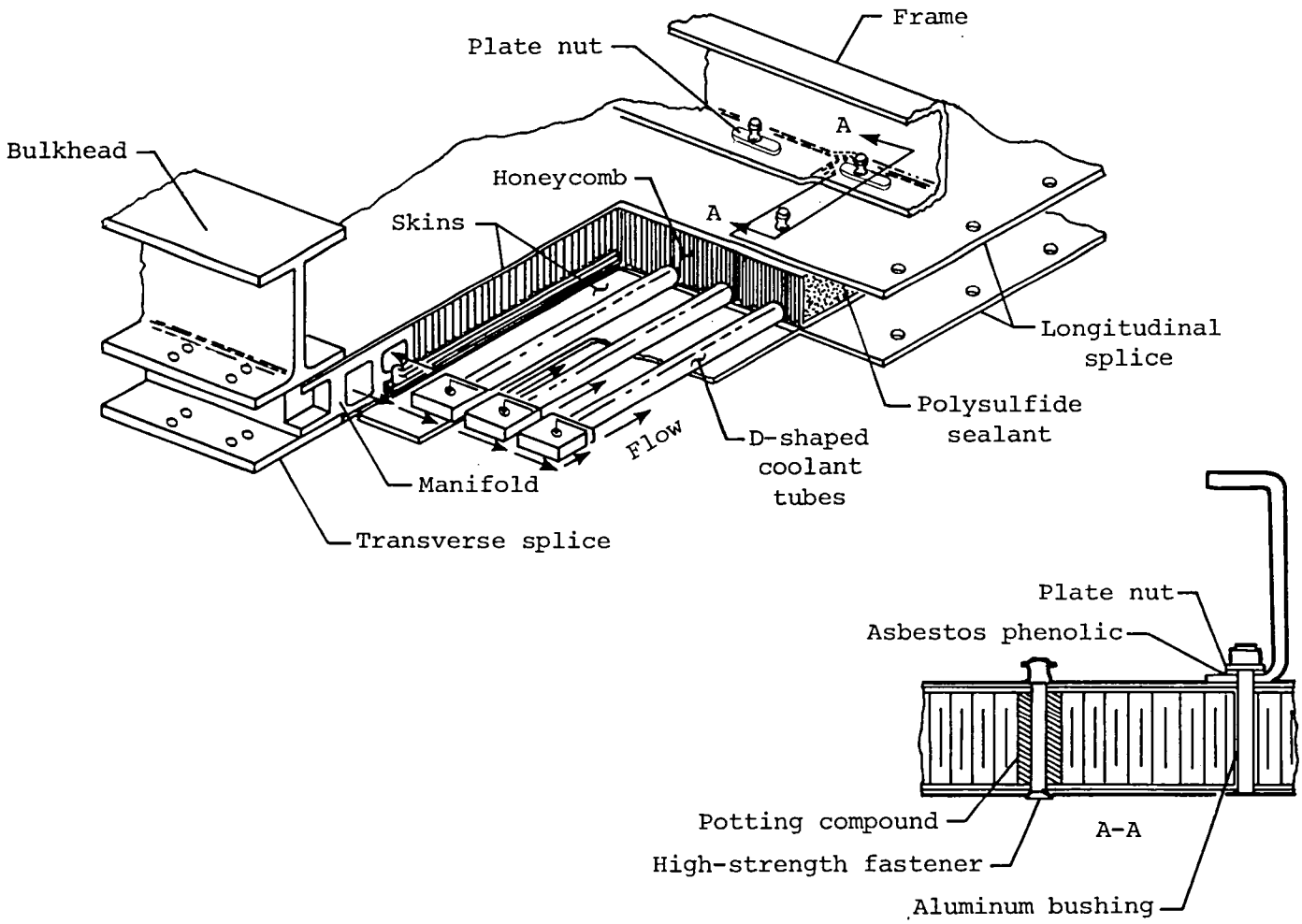

(a) Assembly.

Figure 6.- Details of actively cooled panel.

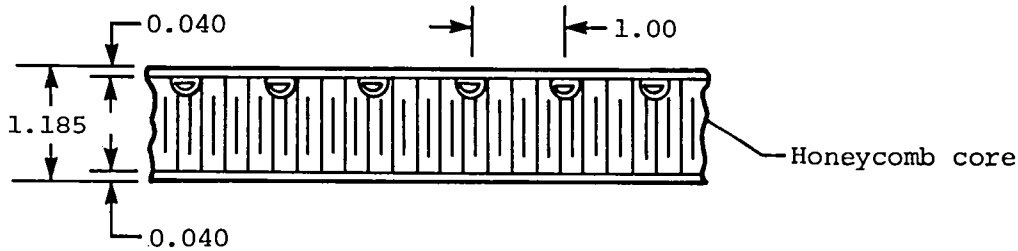

Structural panel

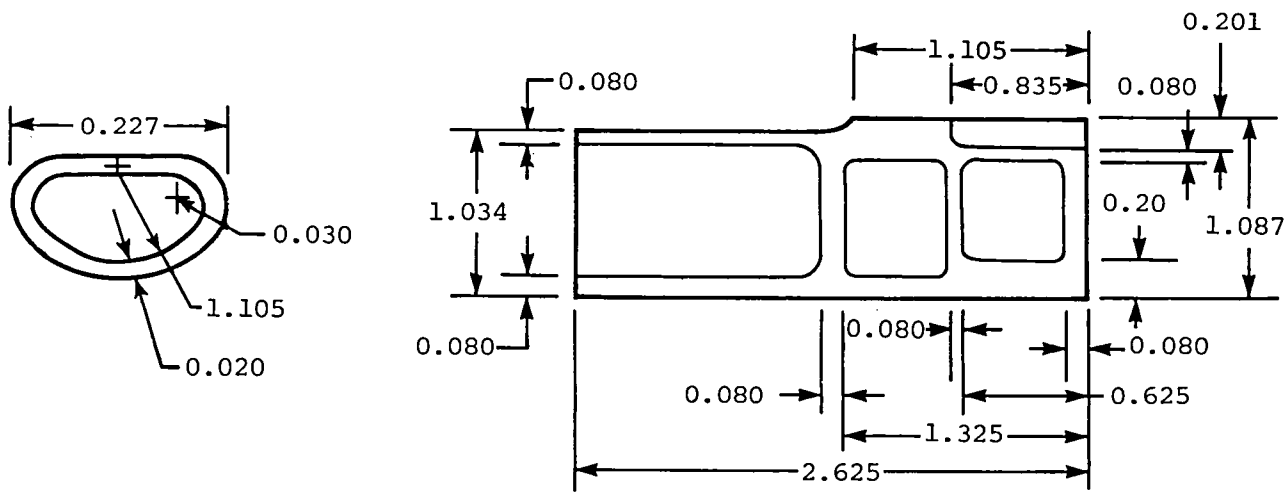

Tube

Manifold

(b) Panel geometry.

Figure 6.- Continued.

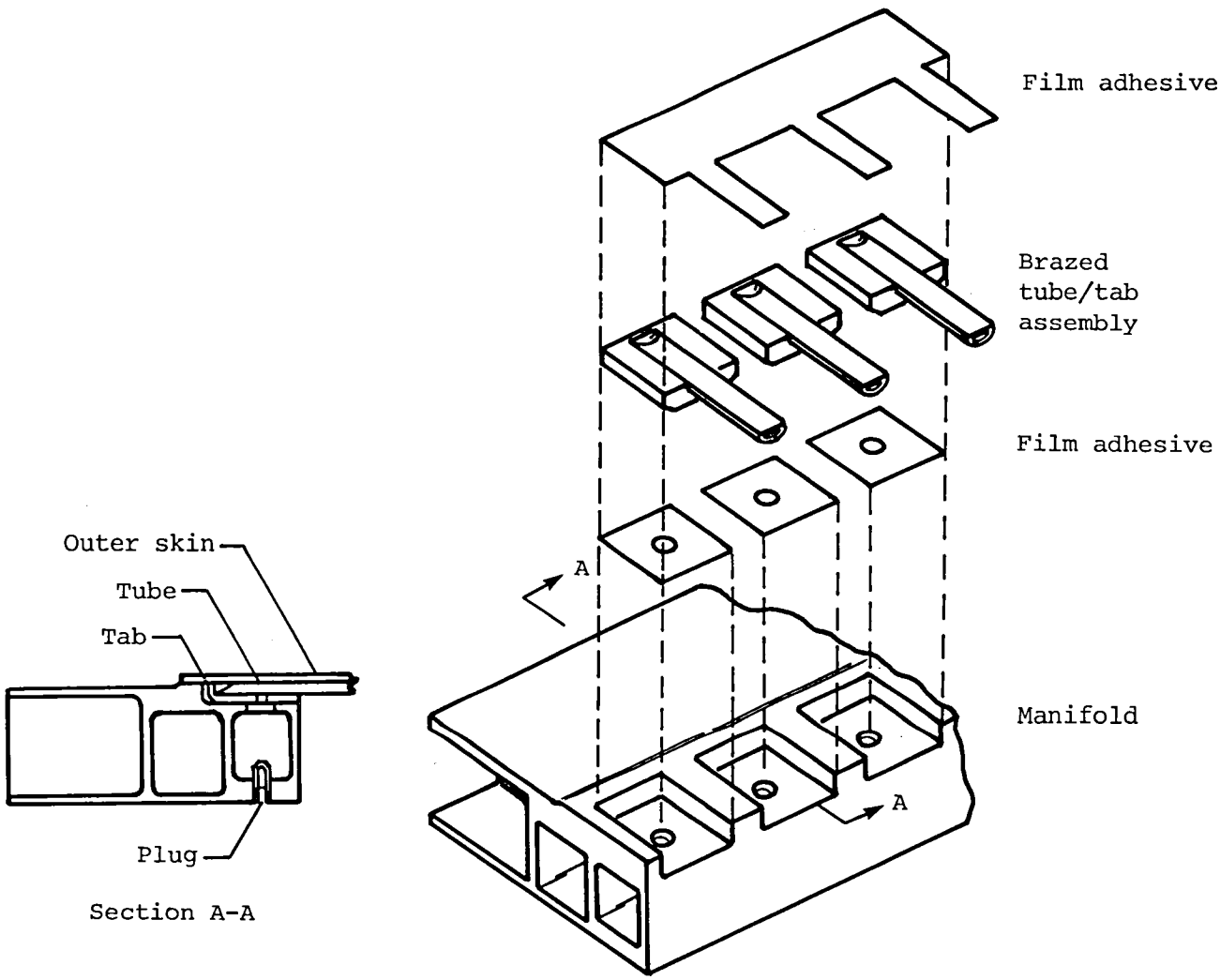

(c) Tube-manifold attachment.

Figure 6.- Concluded.

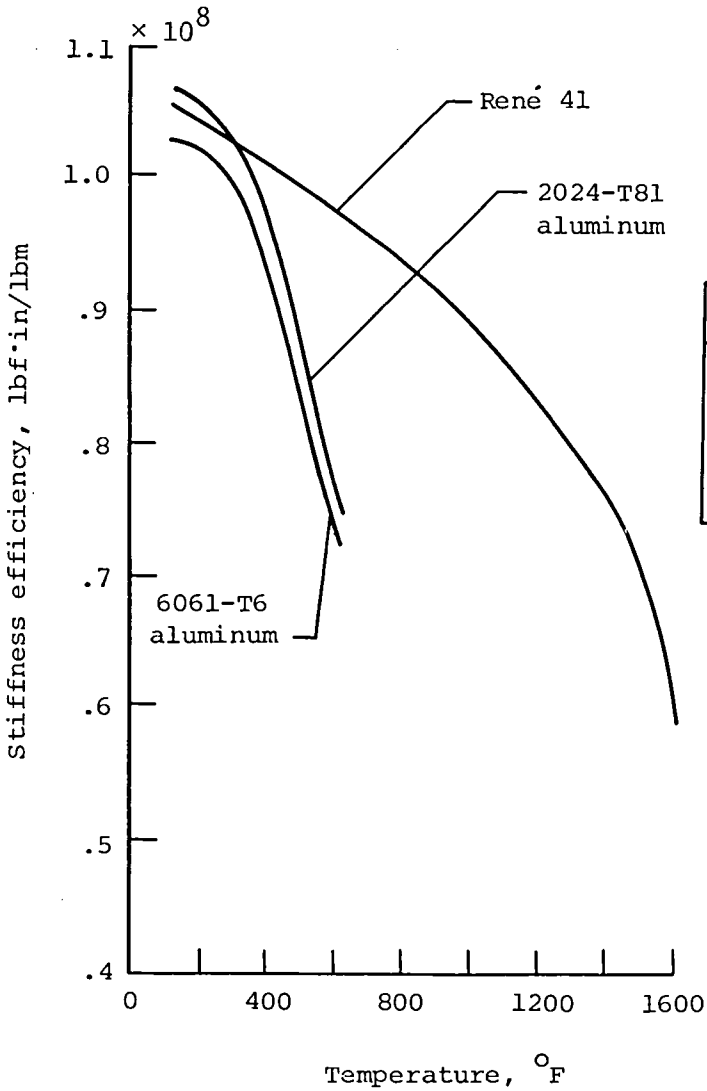

Material	Density, lbm/in^3
René 41 (AMS 5545)	0.298
2024-T81	.100
6061-T6	.098

(a) Stiffness efficiency as function of temperature.

Figure 7.- Properties of metals used in RACP.

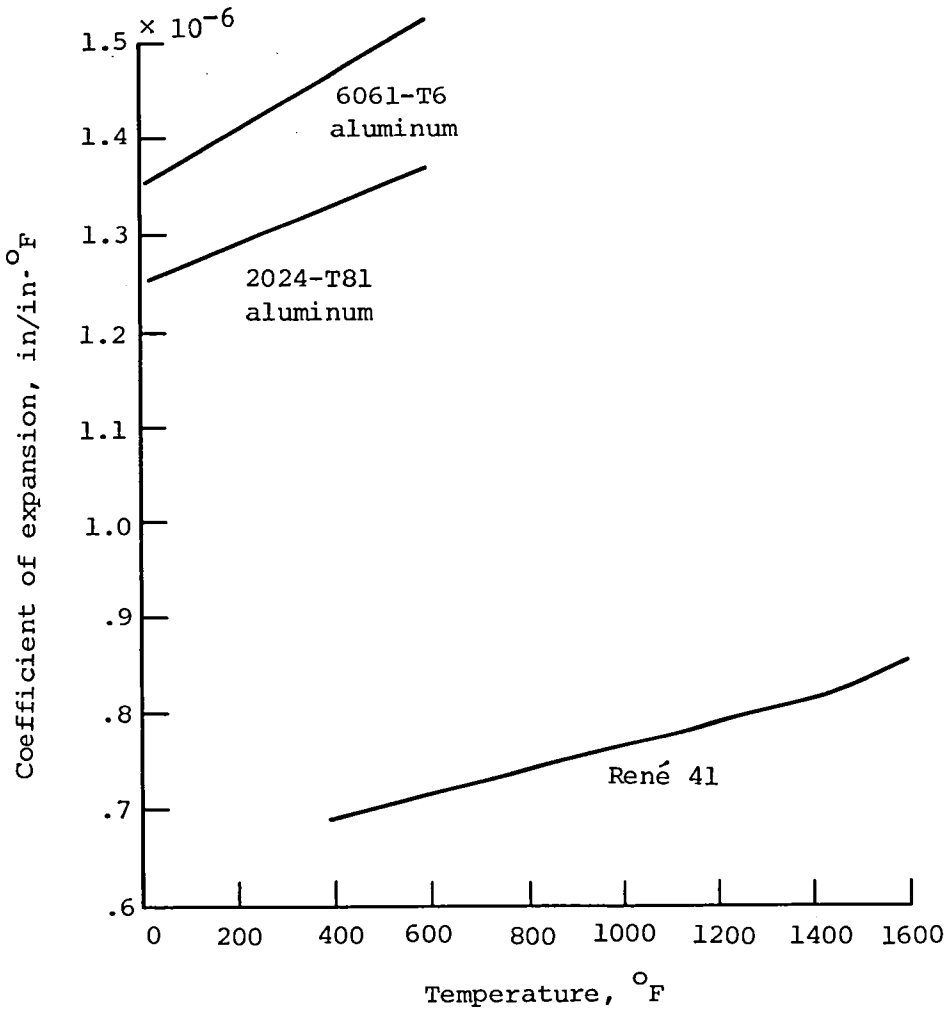

(b) Coefficient of expansion as function of temperature.

Figure 7.- Continued.

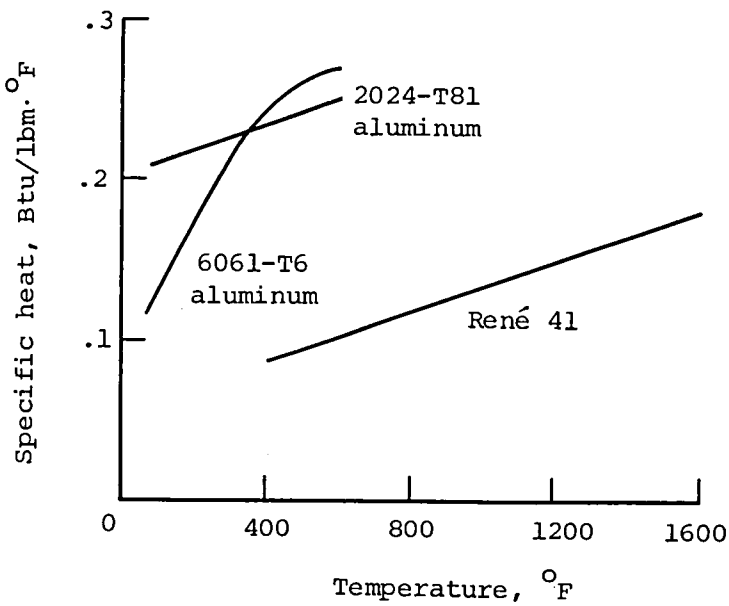

(c) Specific heat as function of temperature.

Figure 7.- Concluded.

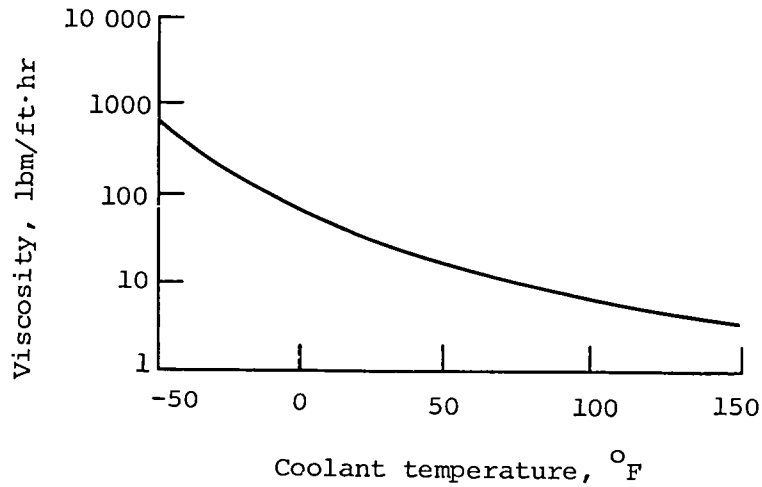

(a) Viscosity as function of temperature for 60-percent mass solution of ethylene glycol in water.

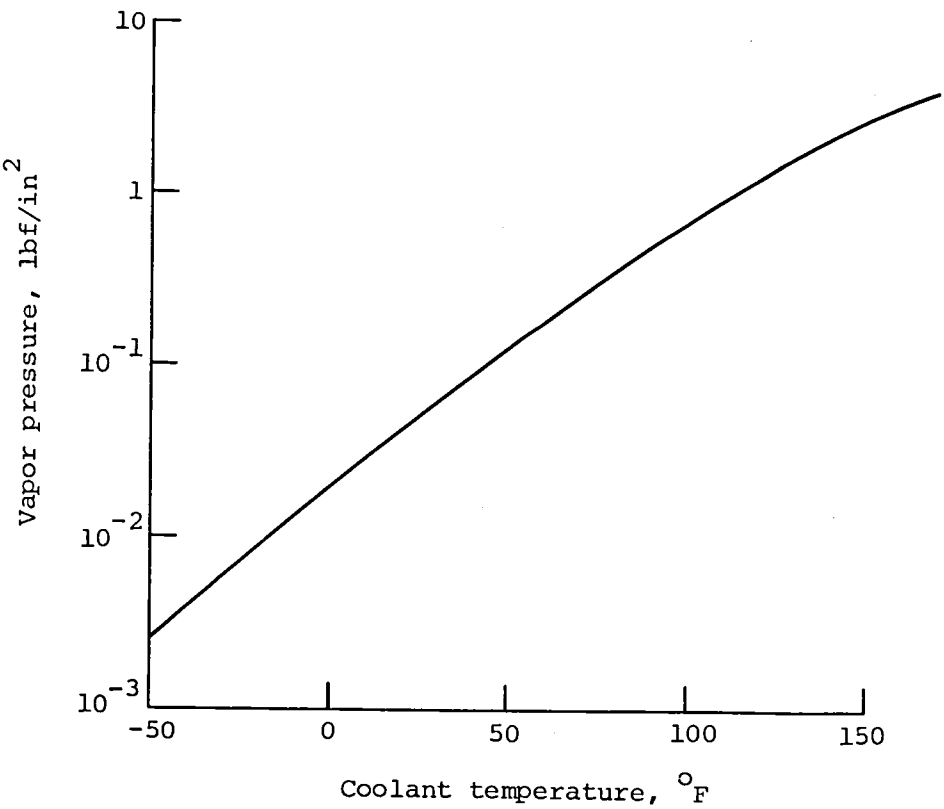

(b) Vapor pressure as function of temperature for 60-percent mass solution of ethylene glycol in water.

Figure 8.- RACP coolant properties.

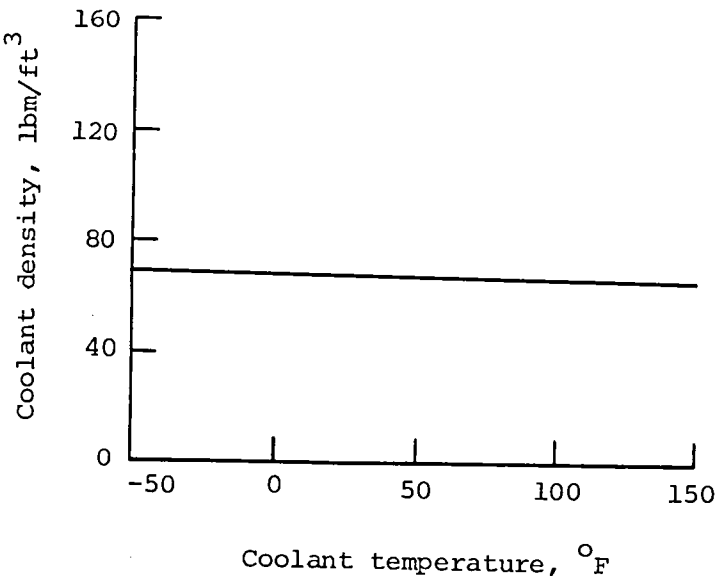

(c) Density as function of temperature for 60-percent mass solution of ethylene glycol in water.

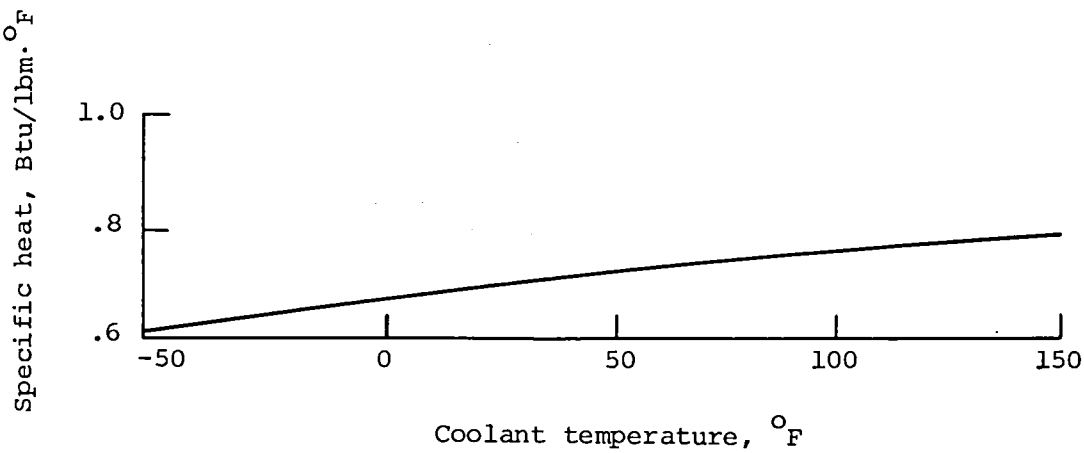

(d) Specific heat as function of temperature for 60-percent mass solution of ethylene glycol in water.

Figure 8.- Continued.

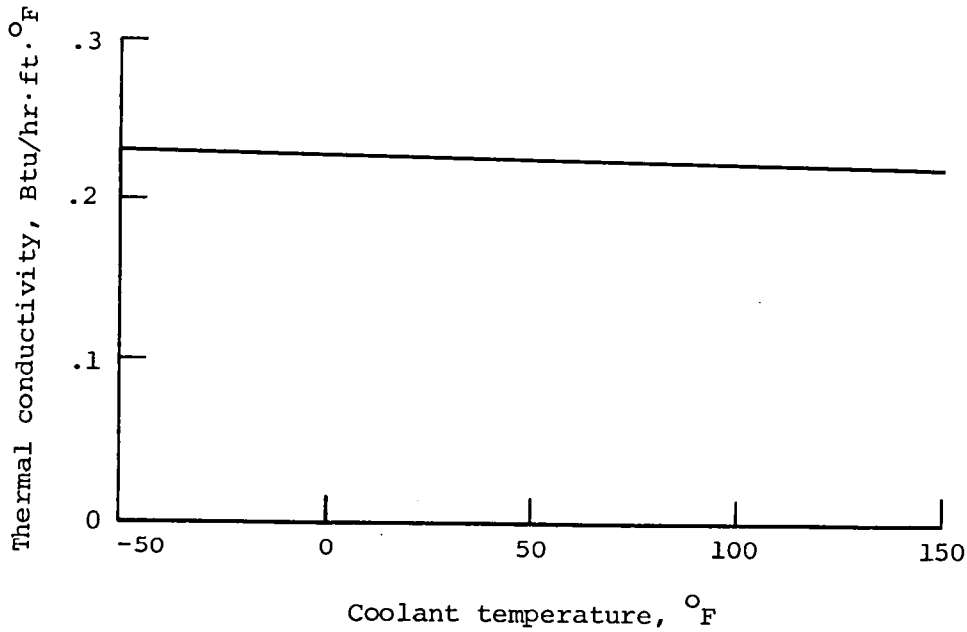

(e) Thermal conductivity as function of temperature for 60-percent mass solution of ethylene glycol in water.

Figure 8.- Concluded.

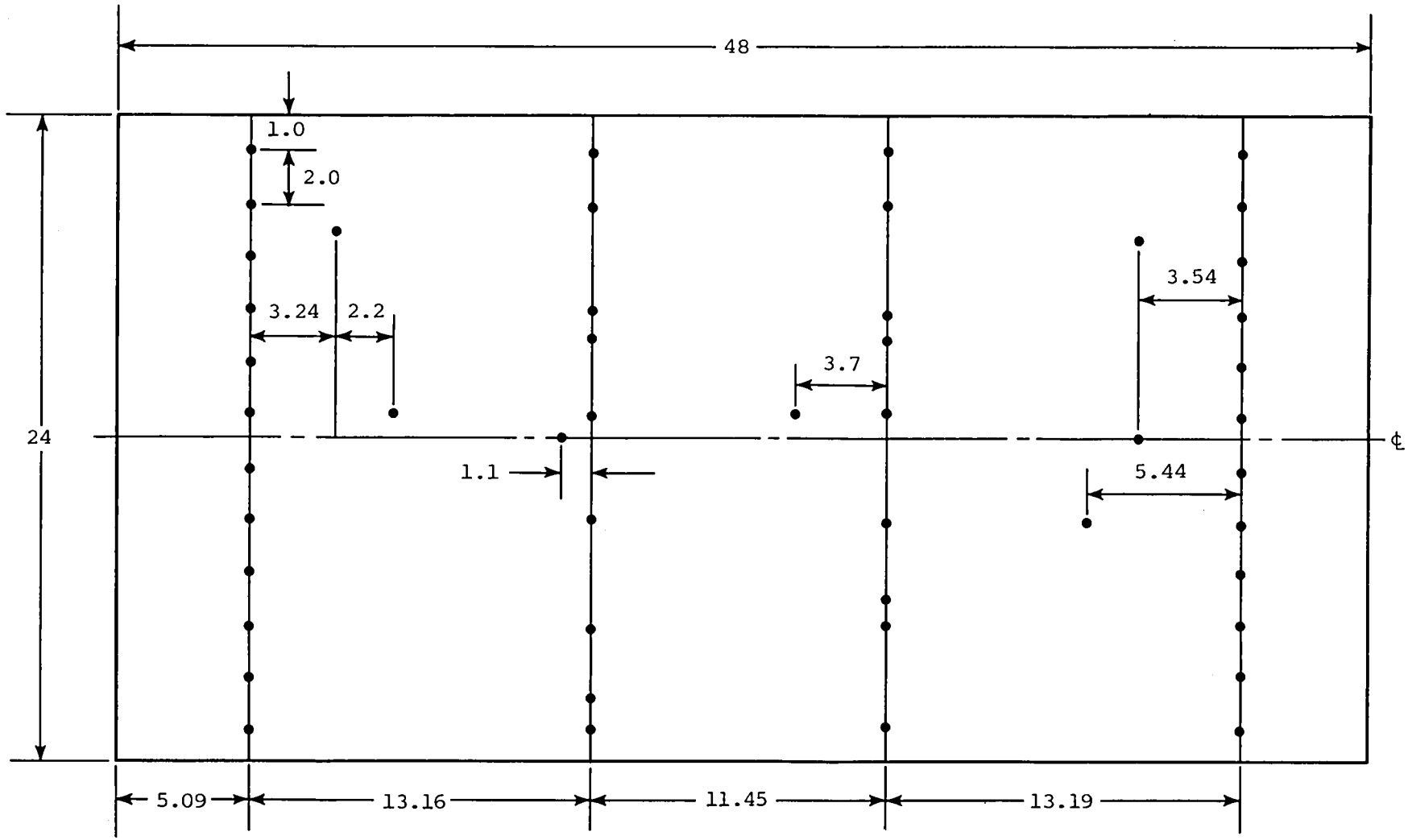

• Thermocouple, corrugated skin

(a) Heat shields.

Figure 9.- RACP instrumentation layout. All dimensions are in inches.

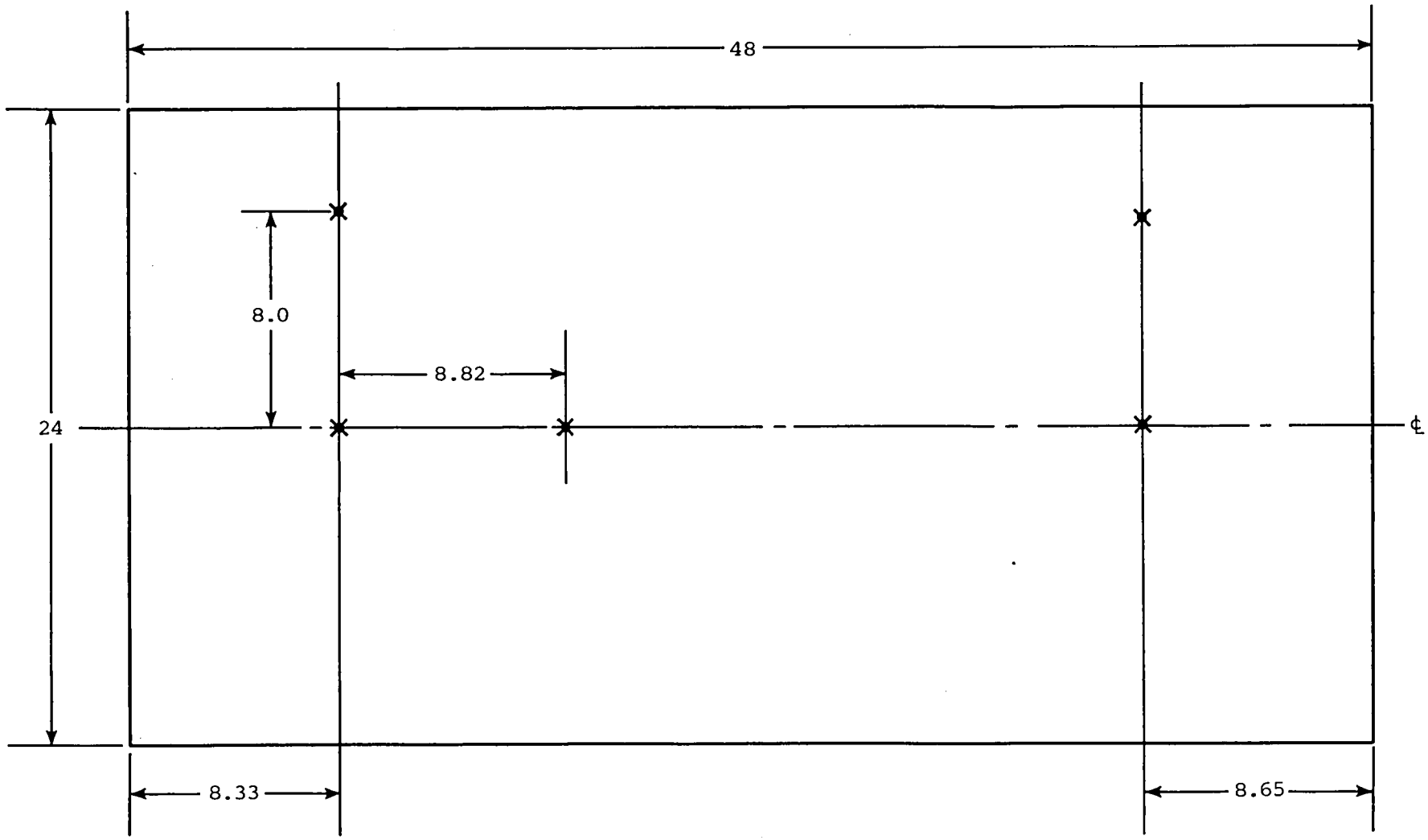

× Thermocouple, heat-shield side

• Thermocouple, structural-panel side

(b) Insulation packages.

Figure 9.- Continued.

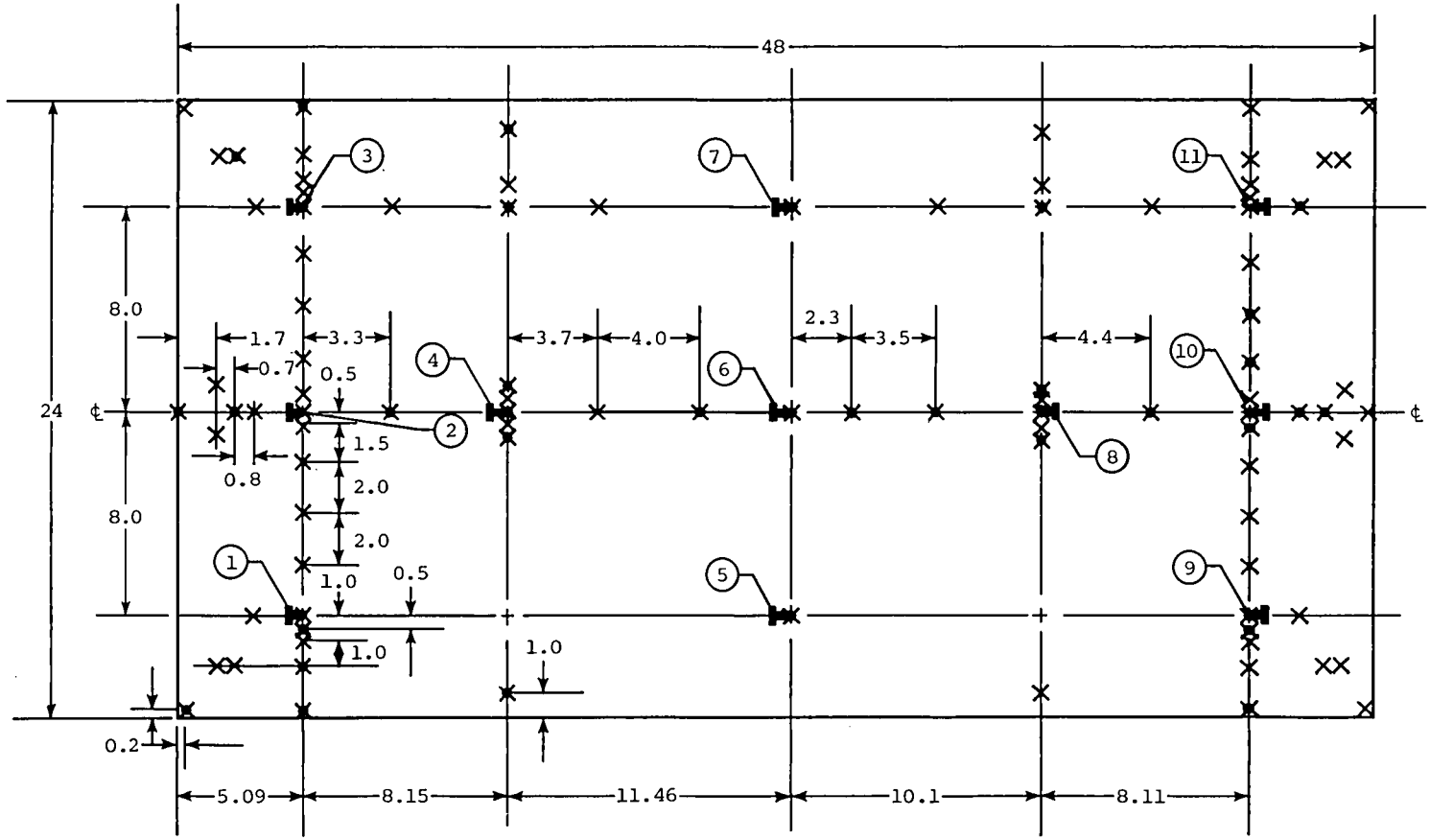

× Thermocouple, outer skin

• Thermocouple, inner skin

▌ Transverse strain gage (T)

▬ Longitudinal strain gage (L)

◯ Strain-gage location

Location	Outer		Inner		Location	Outer		Inner	
	T	L	T	L		T	L	T	L
1	1	2	3	4	7	25	26	27	28
2	5	6	7	8	8	29	30	31	32
3	9	10	11	12	9	33	34	35	36
4	13	14	15	16	10	37	38	39	40
5	17	18	19	20	11	41	42	43	44
6	21	22	23	24					

Strain-gage number sequence

(c) Structural panel.

Figure 9.- Concluded.

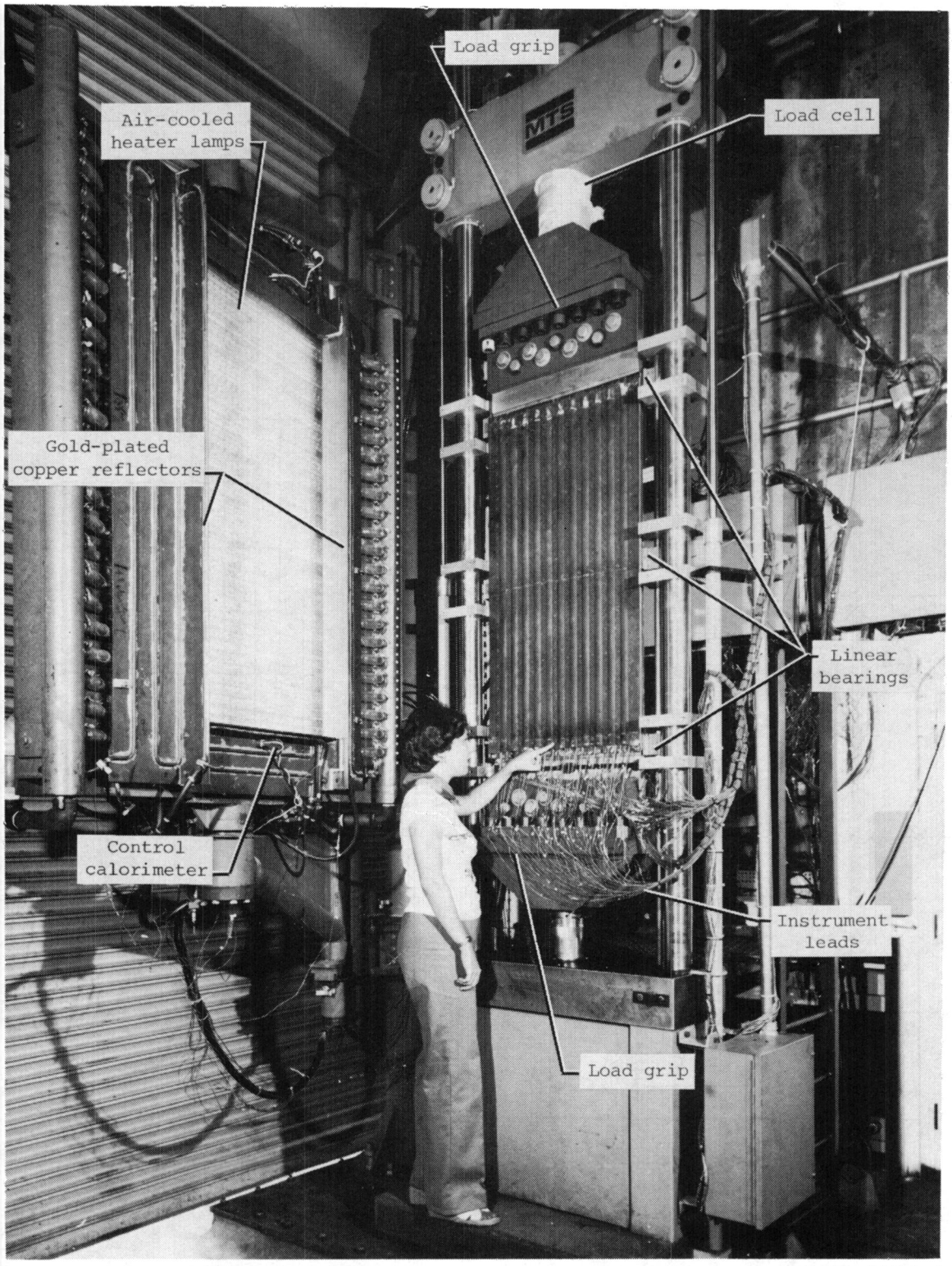

L-79-4298.1

Figure 10.- Active-cooling test stand (ACTS) with test panel.

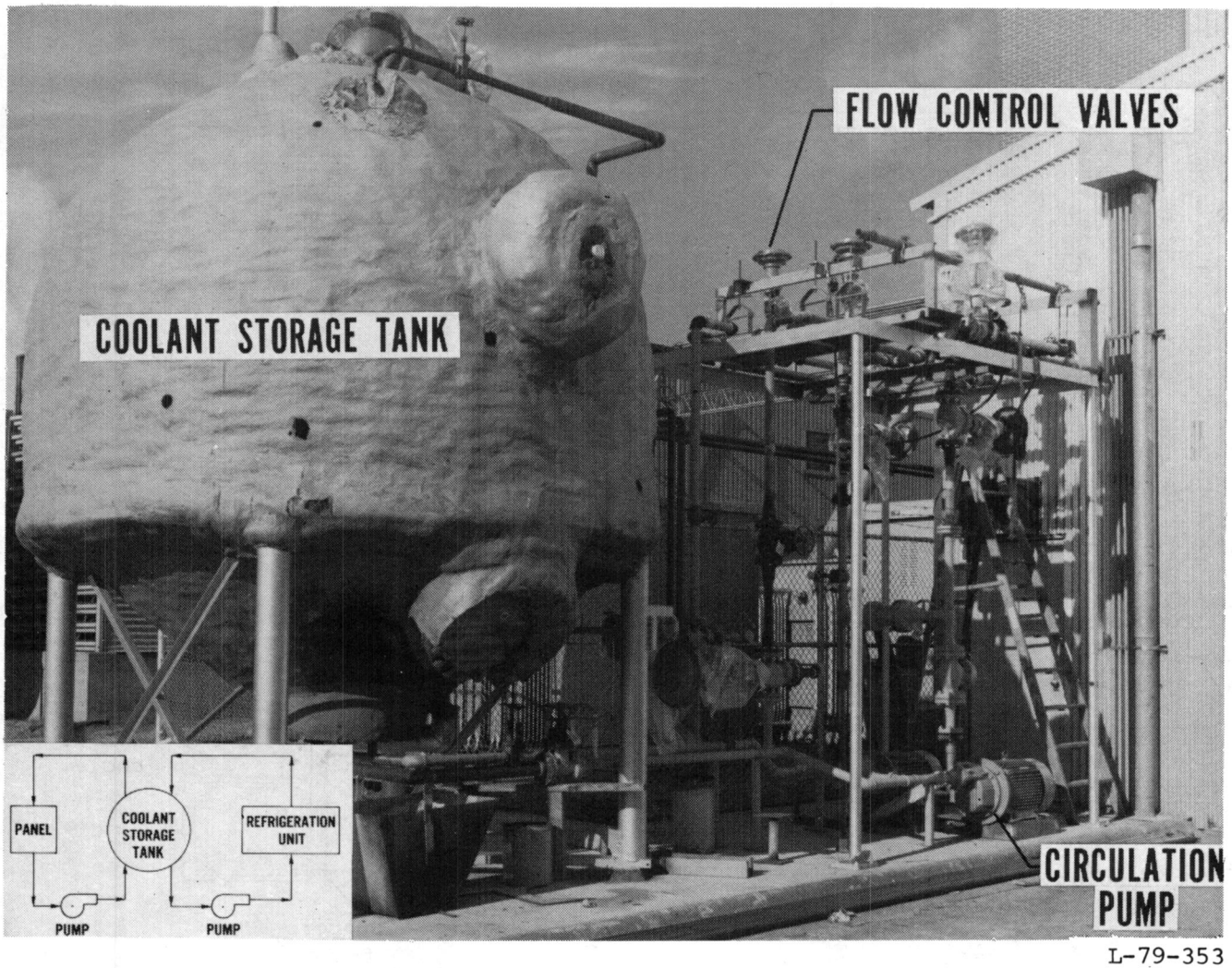

L-79-353

Figure 11.- ACTS cooling system.

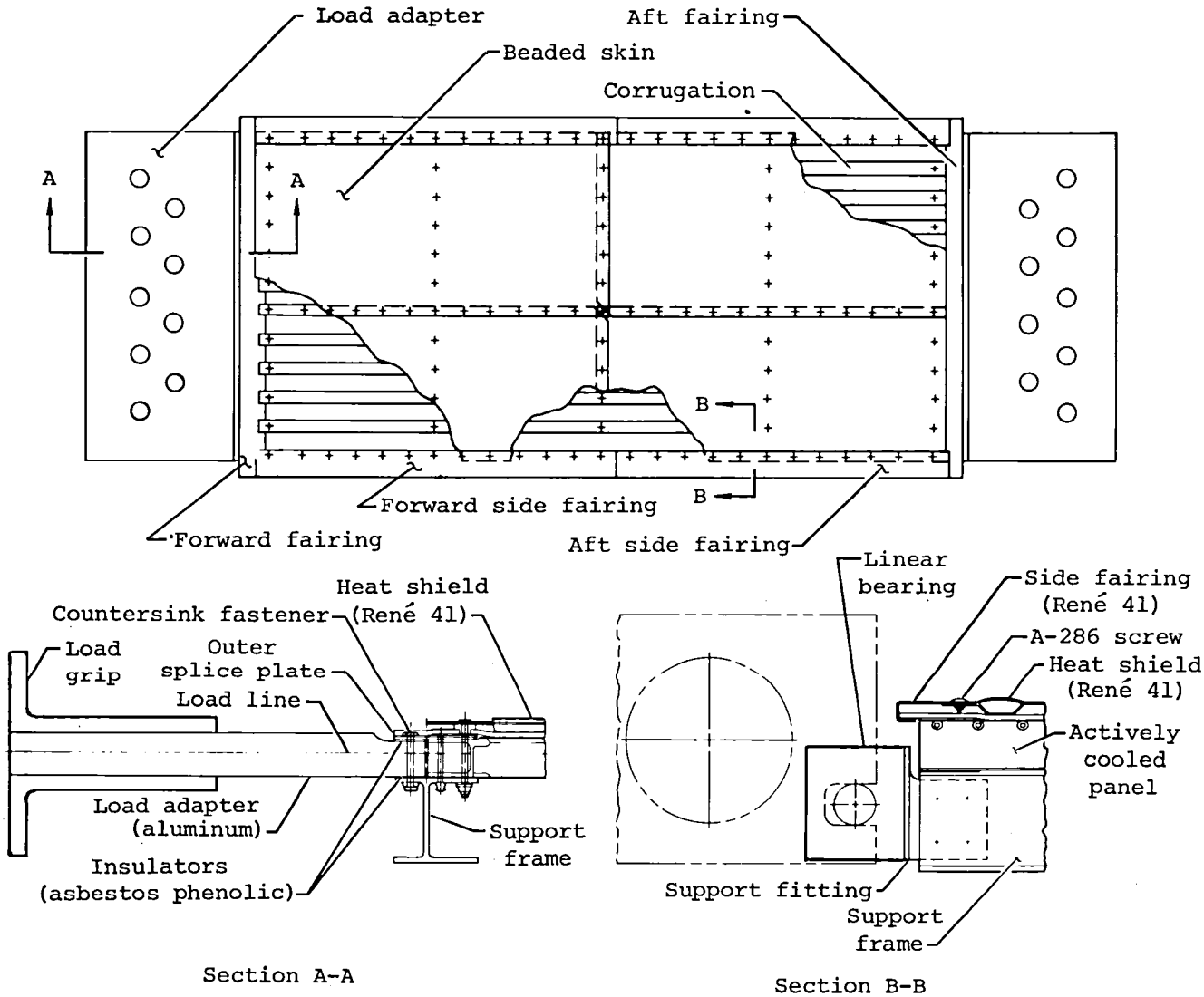

Figure 12.- Details of RACP mounting arrangement for ACTS.

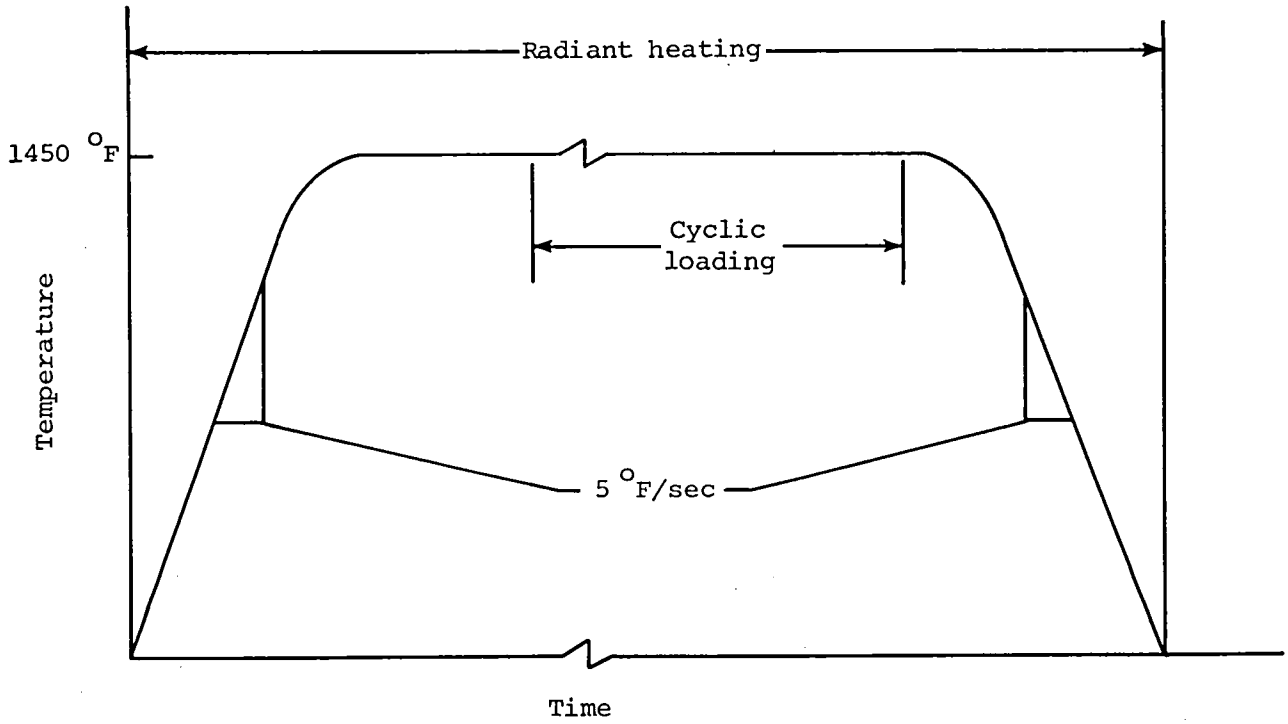

Figure 13.- Typical surface temperature history.

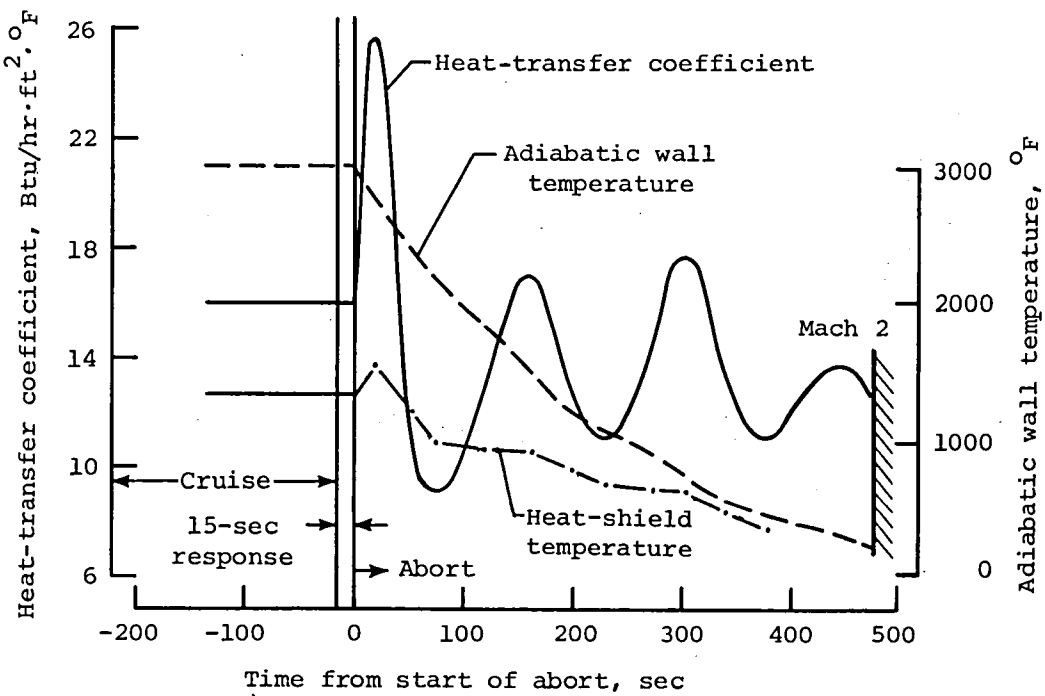

Figure 14.- Abort heating profile.

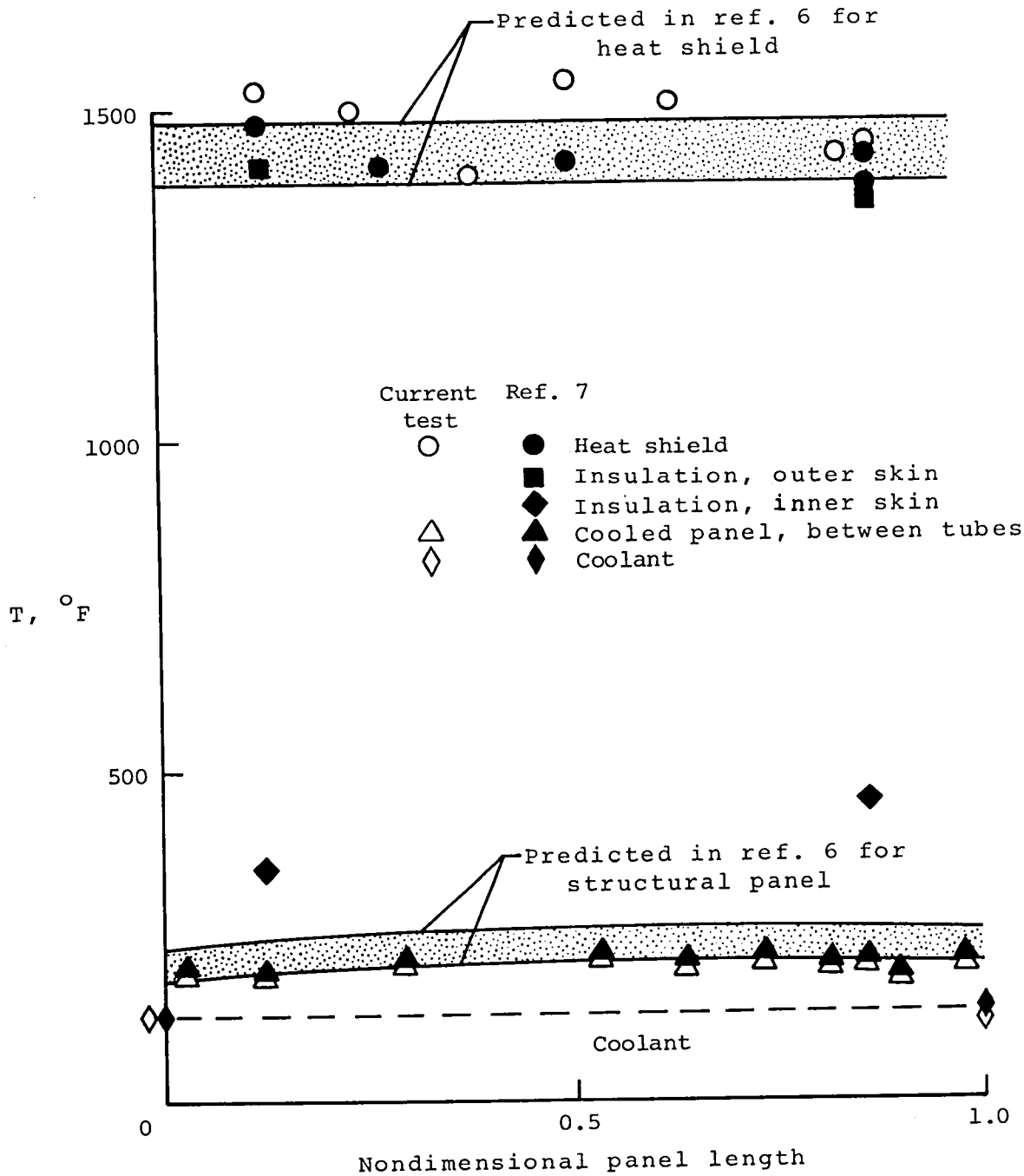

Figure 15.- Comparison of longitudinal RACP temperature distributions from current radiant heating tests with comparable tests from reference 7.

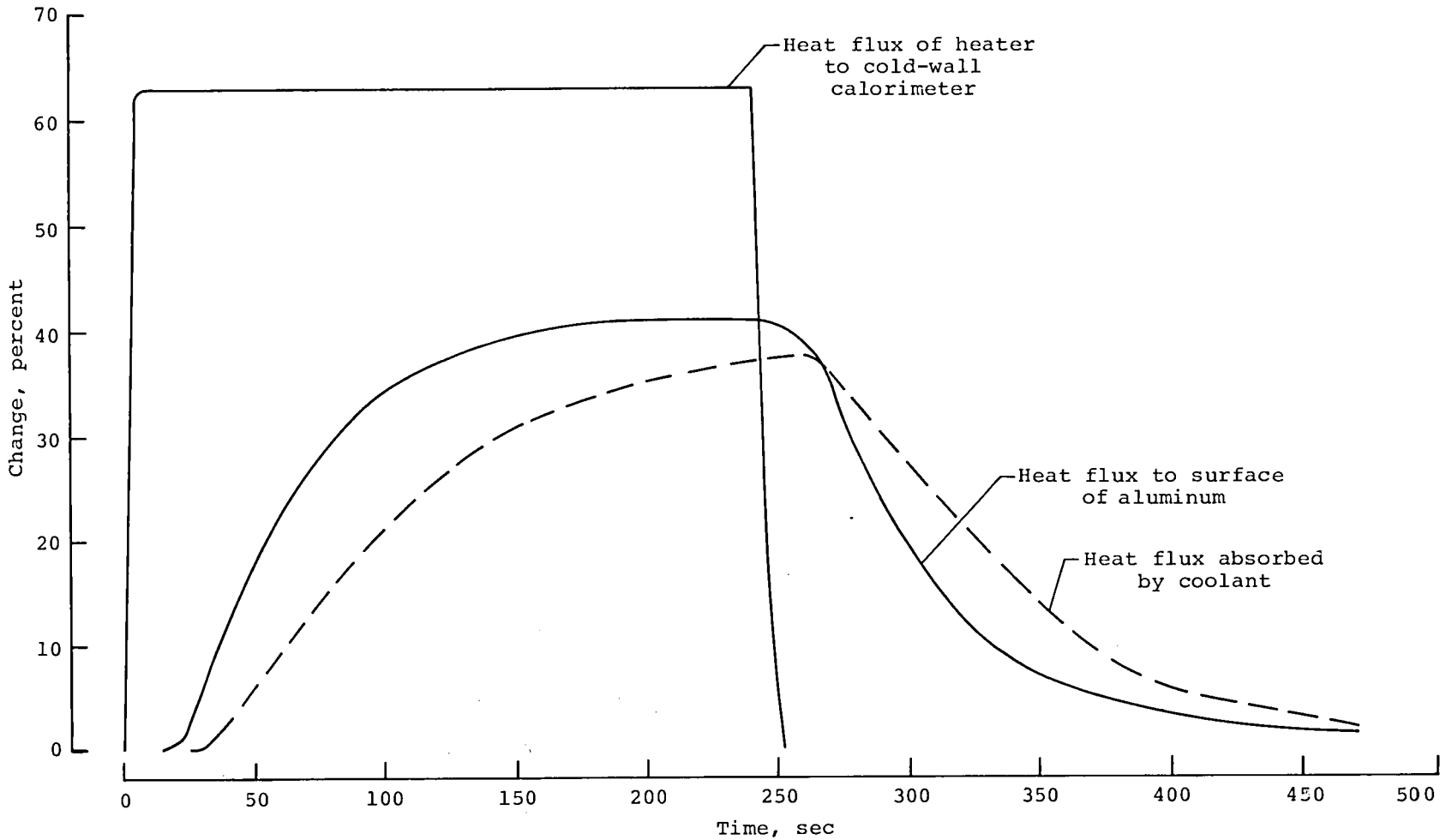

Figure 16.- Applied heating for maneuver and cooled-panel heat-flux response.

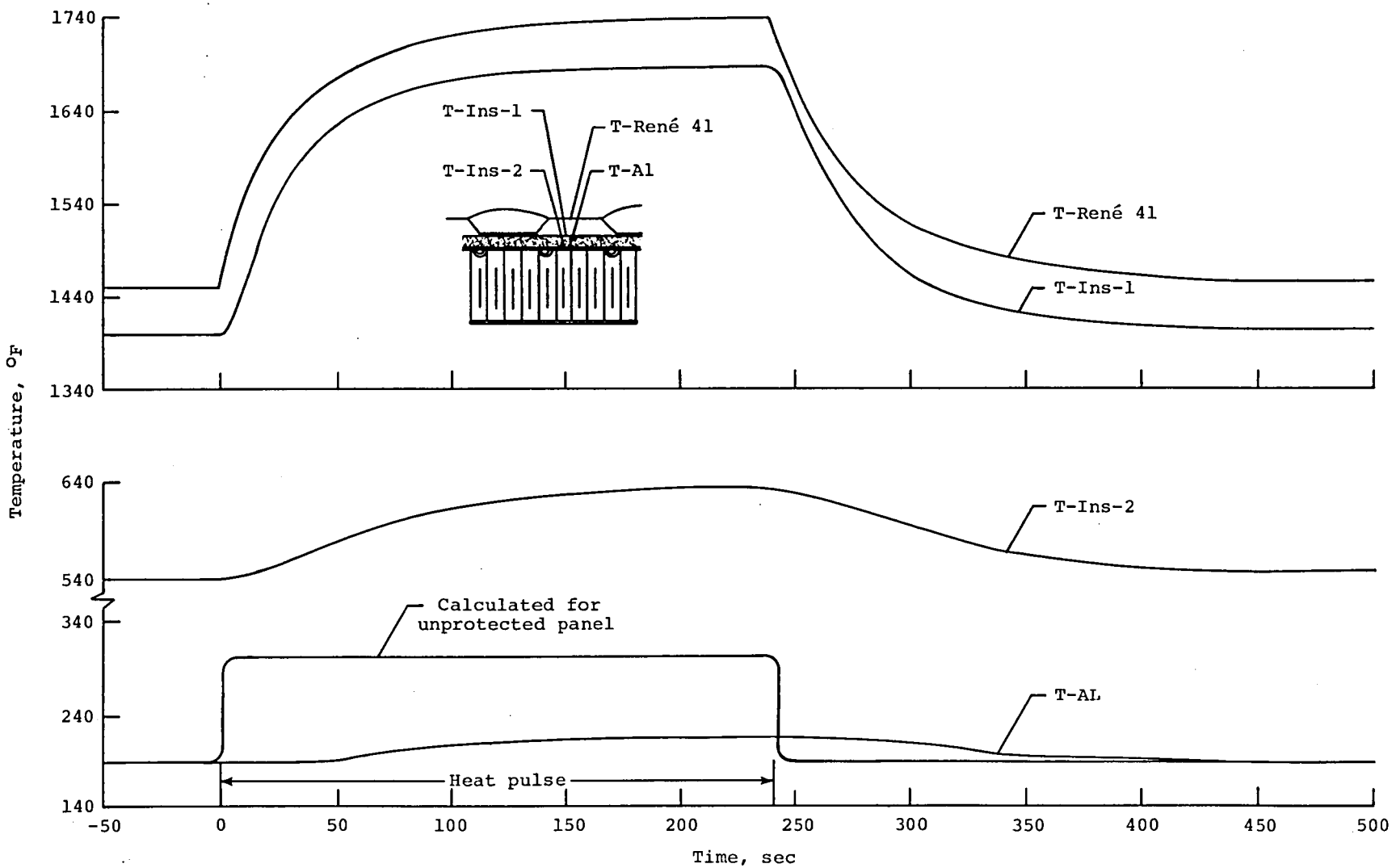

Figure 17.- Temperature response of RACP to maneuver heating.

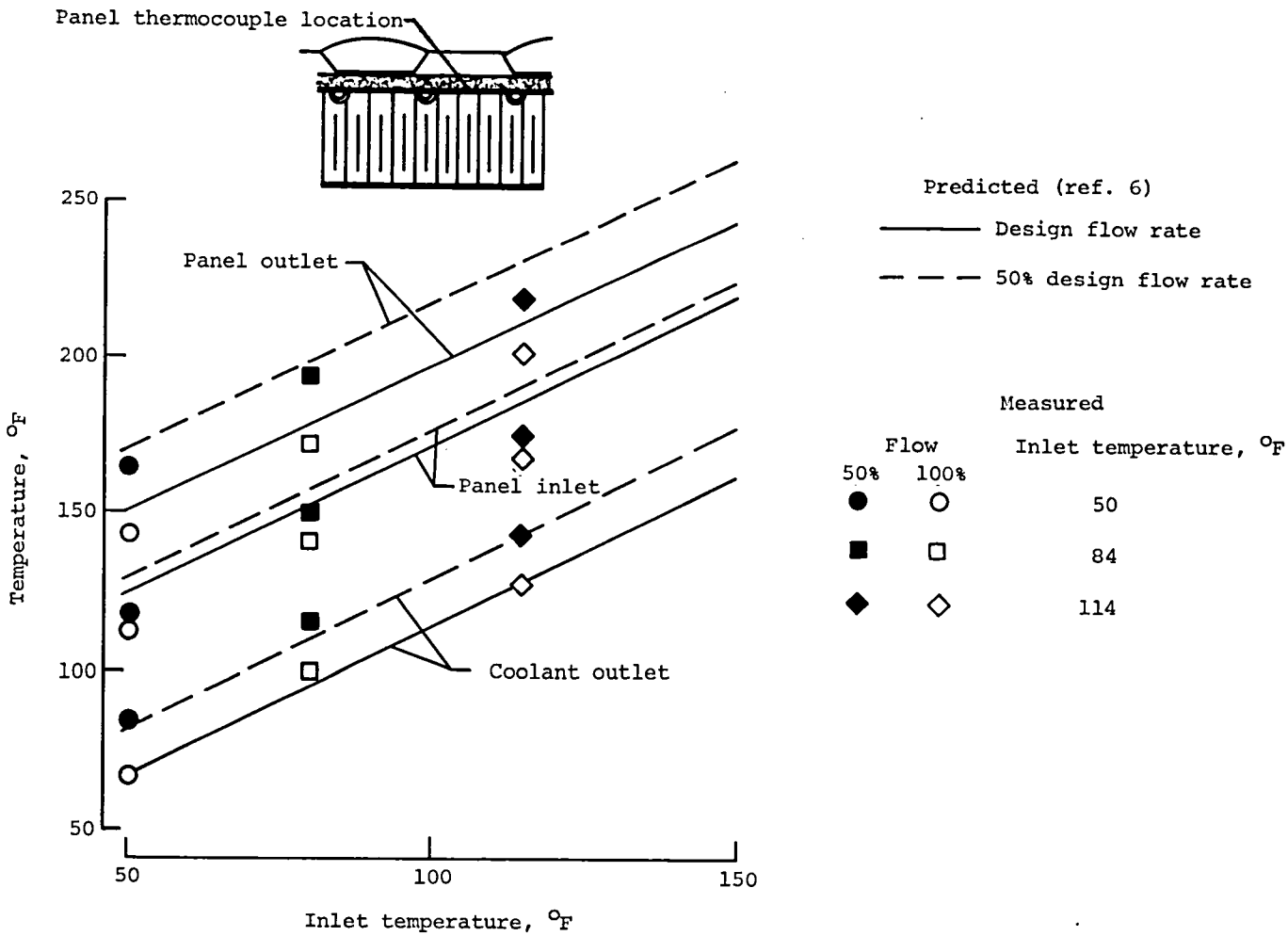

Figure 18.- Effect of inlet coolant temperature and flow rate on temperatures of RACP cooled panel.

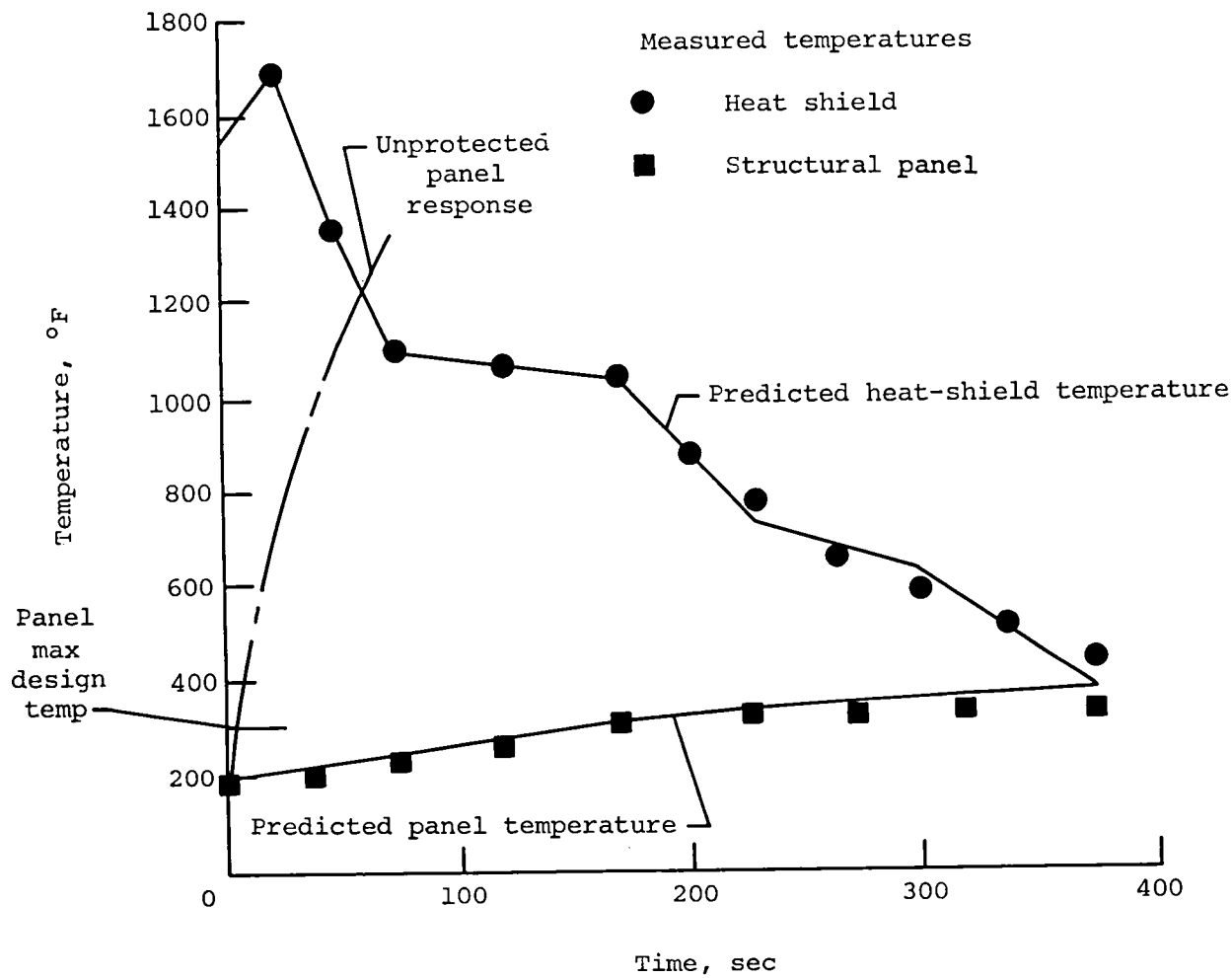

Figure 19.- RACP response to abort heating.

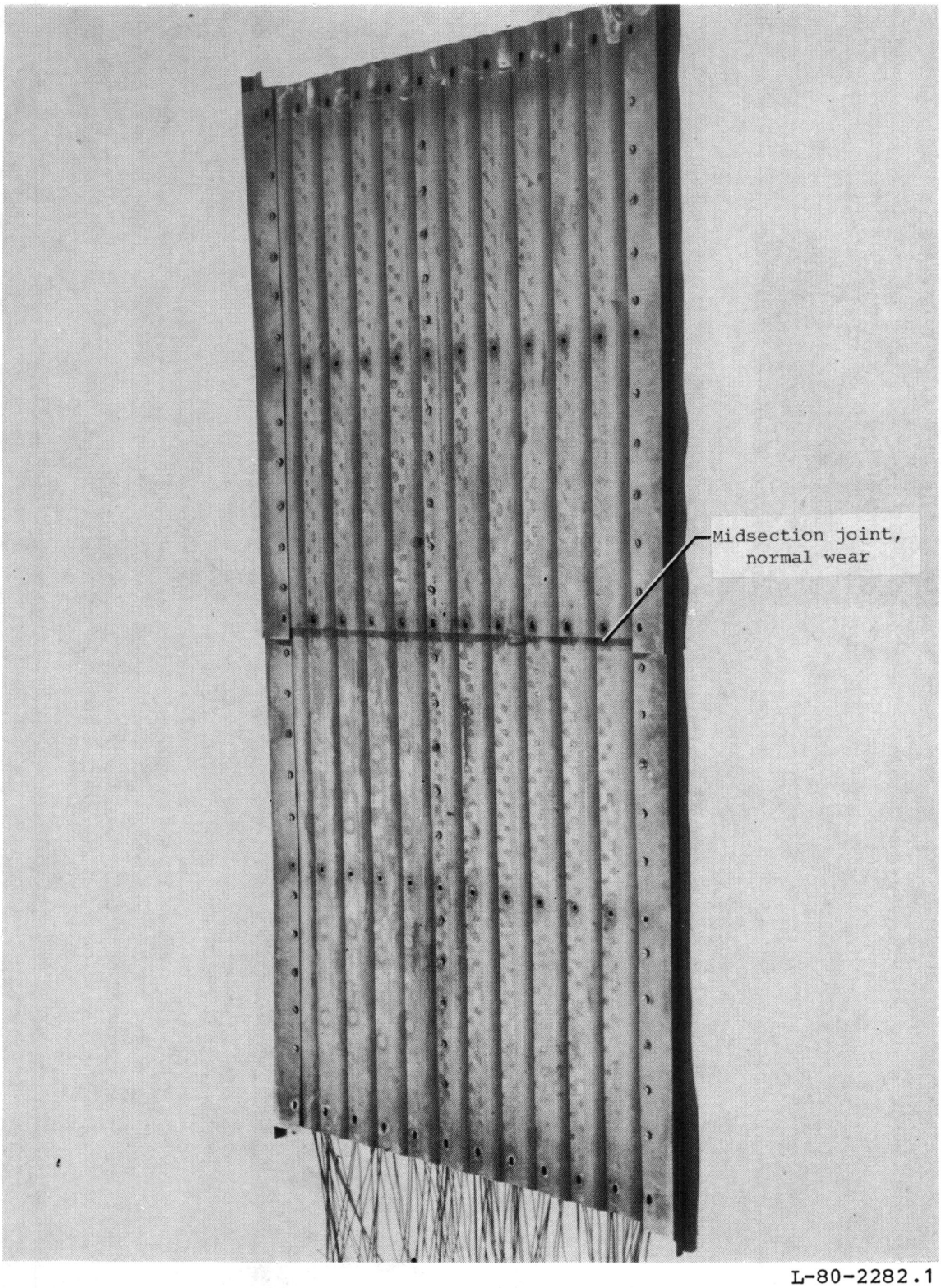

(a) Beaded skin.

Figure 20.- Posttest condition of RACP heat shield.

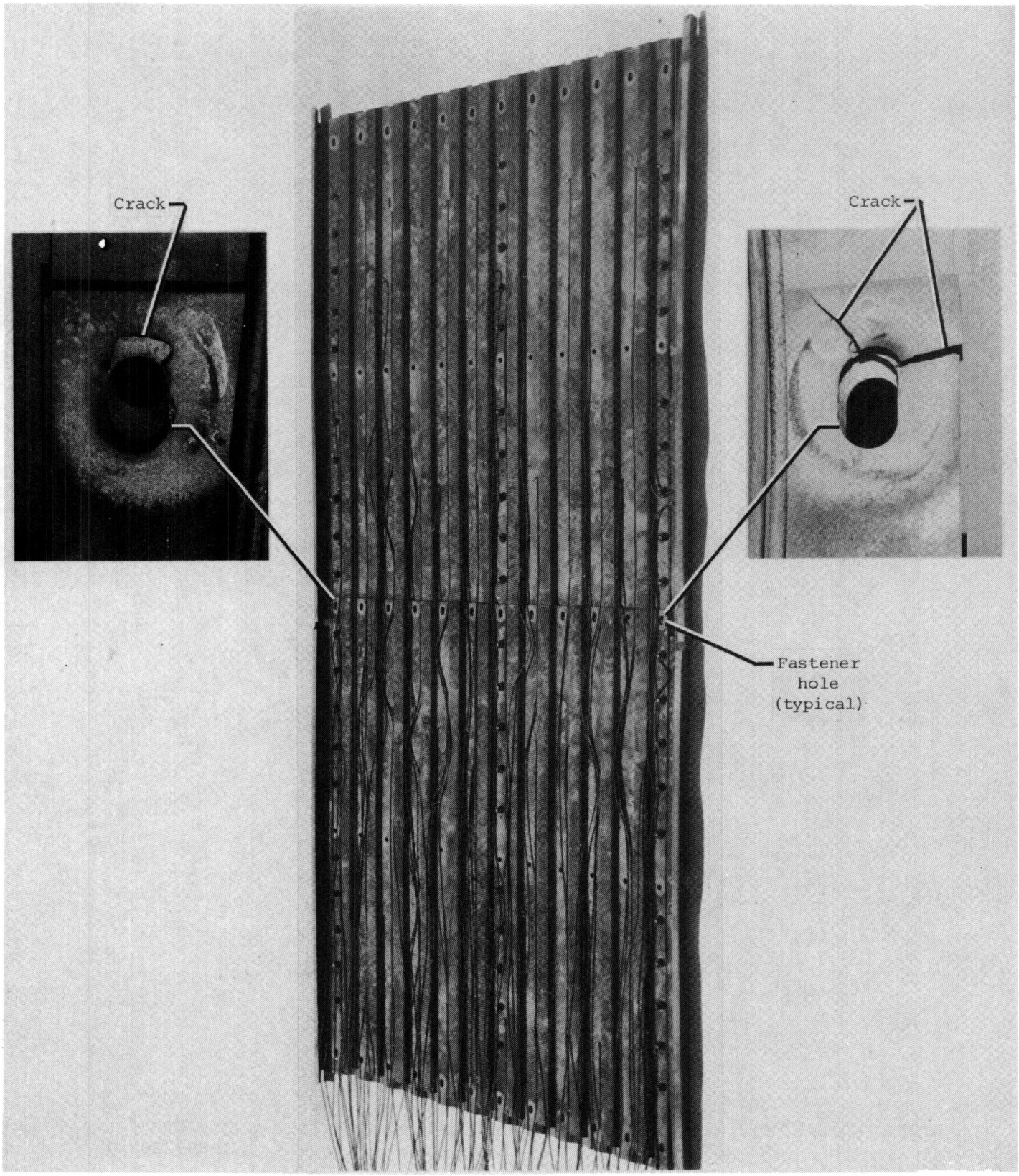

(b) Corrugated skin.

Figure 20.- Concluded.

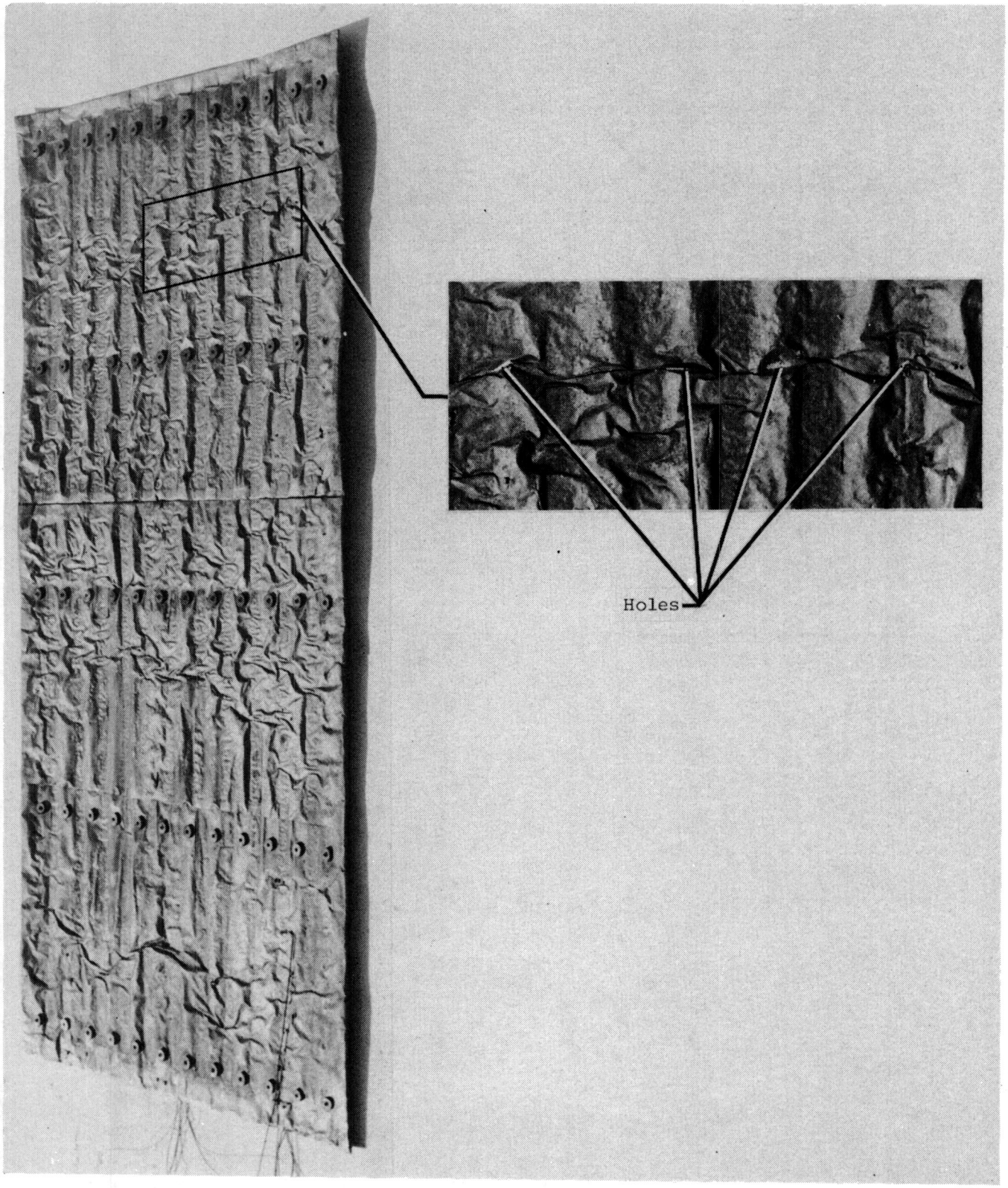

(a) Heat-shield side.

Figure 21.- Posttest condition of insulation package.

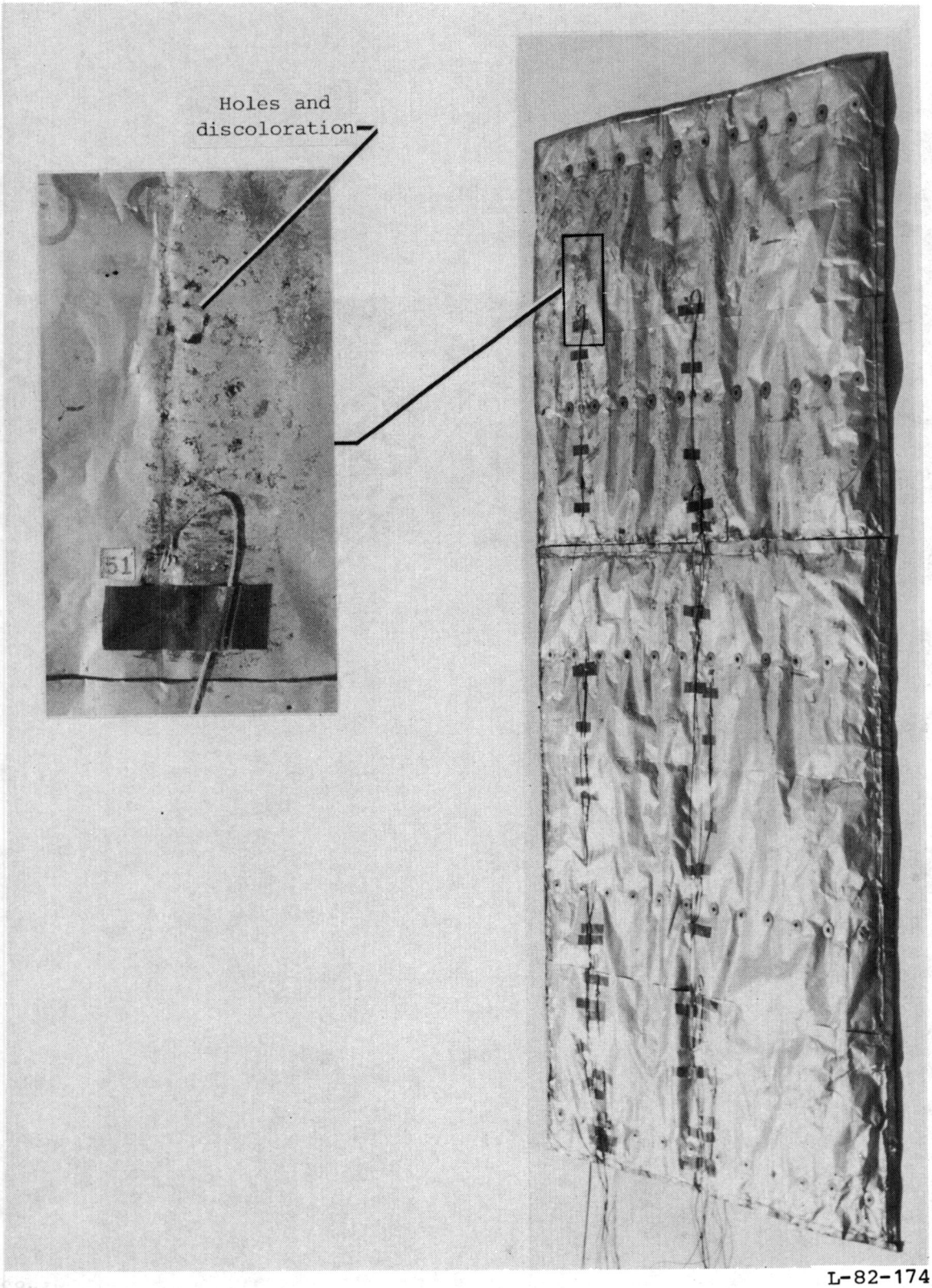

(b) Structural panel side.

Figure 21.- Concluded.

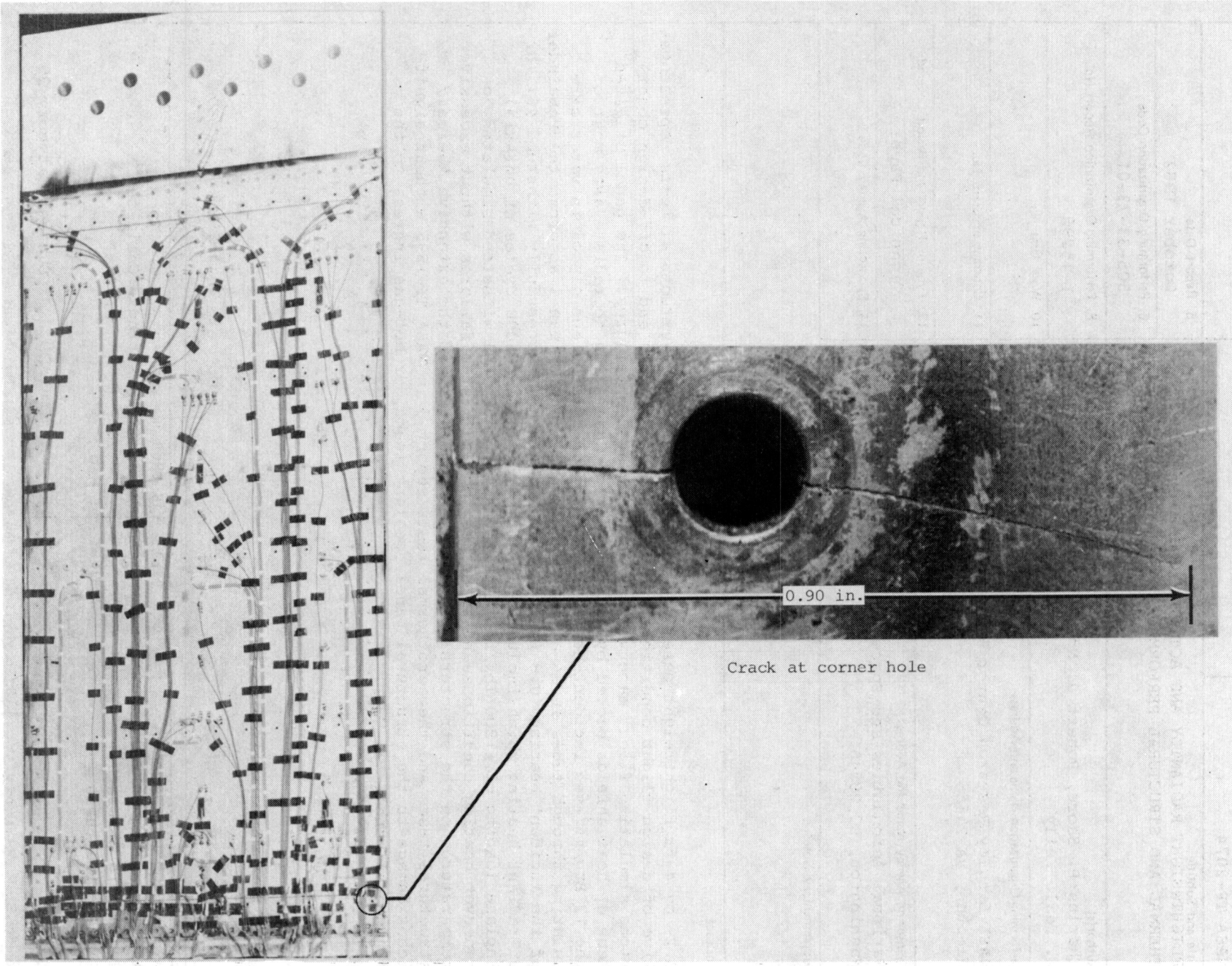

Figure 22.- Posttest condition of structural panel, heated side.

1. Report No.	2. Government Accession No.	3. Recipient's Catalog No.
NASA TP-2074		

4. Title and Subtitle	5. Report Date
FLIGHTWEIGHT RADIANTLY AND ACTIVELY COOLED PANEL - THERMAL AND STRUCTURAL PERFORMANCE	October 1982
	6. Performing Organization Code 505-33-73-01

7. Author(s)	8. Performing Organization Report No.
Charles P. Shore, Robert J. Nowak, and H. Neale Kelly	L-15292
	10. Work Unit No.

9. Performing Organization Name and Address	11. Contract or Grant No.
NASA Langley Research Center Hampton, VA 23665	
	13. Type of Report and Period Covered Technical Paper

12. Sponsoring Agency Name and Address	14. Sponsoring Agency Code
National Aeronautics and Space Administration Washington, DC 20546	

15. Supplementary Notes

16. Abstract

A 2- by 4-ft flightweight panel was subjected to thermal/structural tests representative of design flight conditions for a Mach 6.7 transport and to off-design conditions simulating flight maneuvers and cooling system failures. The panel utilized René 41 heat shields backed by a thin layer of insulation to radiate away most of the 12 Btu/ft^2-sec incident heating. A solution of ethylene glycol in water circulating through tubes in an aluminum-honeycomb-sandwich panel absorbed the remainder of the incident heating (0.8 Btu/ft^2-sec). The panel successfully withstood 46.7 hr of radiant heating which included 53 thermal cycles and 5000 cycles of uniaxial inplane loading of ±1200 lbf/in. Additionally, the panel withstood simulated 2g-maneuver heating conditions and simulated cooling system failures without excessive temperatures on the structural panel. The panel survived the extensive thermal/structural tests and the aerothermal tests reported in NASA TP-1595 without significant damage to the structural panel, coolant leaks, or hot-gas ingress to the structural panel.

17. Key Words (Suggested by Author(s))	18. Distribution Statement
Active cooling Hypersonic aircraft Heated structures	Unclassified - Unlimited Subject Category 39

19. Security Classif. (of this report)	20. Security Classif. (of this page)	21. No. of Pages	22. Price
Unclassified	Unclassified	51	A04

For sale by the National Technical Information Service, Springfield, Virginia 22161

NASA-Langley, 1982

National Aeronautics and
Space Administration

Washington, D.C.
20546

Official Business
Penalty for Private Use, $300

THIRD-CLASS BULK RATE

Postage and Fees Paid
National Aeronautics and
Space Administration
NASA-451

NASA

POSTMASTER: If Undeliverable (Section 158 Postal Manual) Do Not Return